J. Mech. Phys. Solids 154 (2021) 104544

Contents lists available at ScienceDirect

Journal of the Mechanics and Physics of Solids

journal homepage: www.elsevier.com/locate/jmps

The nonlinear viscoelastic response of suspensions of rigid inclusions in rubber: I—Gaussian rubber with constant viscosity

Kamalendu Ghosh, Bhavesh Shrimali, Aditya Kumar, Oscar Lopez-Pamies *

Department of Civil and Environmental Engineering, University of Illinois, Urbana–Champaign, IL 61801, USA

ARTICLE INFO

Keywords:
Elastomers
Fillers
Finite deformation
Homogenization
Reinforcement

ABSTRACT

A numerical and analytical study is made of the macroscopic or homogenized viscoelastic response of suspensions of rigid inclusions in rubber under finite quasistatic deformations. The focus is on the prototypical case of random isotropic suspensions of equiaxed inclusions firmly embedded in an isotropic incompressible Gaussian rubber with constant viscosity. From a numerical point of view, a robust scheme is introduced to solve the governing initial–boundary-value problem based on a conforming Crouzeix–Raviart finite-element discretization of space and a high-order accurate explicit Runge–Kutta discretization of time, which are particularly well suited to deal with the challenges posed by finite deformations and the incompressibility constraint of the rubber. The scheme is deployed to generate sample solutions for the basic case of suspensions of spherical inclusions of the same (monodisperse) size under a variety of loading conditions. From a complementary point of view, analytical solutions are worked out in the limits: (*i*) of small deformations, (*ii*) of finite deformations that are applied either infinitesimally slowly or infinitely fast, and (*iii*) when the rubber loses its ability to store elastic energy and reduces to a Newtonian fluid. Strikingly, in spite of the fact that the underlying rubber matrix has constant viscosity, the solutions reveal that the viscoelastic response of the suspensions exhibits an effective nonlinear viscosity of shear-thinning type. The solutions further indicate that the viscoelastic response of the suspensions features the same type of short-range-memory behavior — as opposed to the generally expected long-range-memory behavior — as that of the underlying rubber. Guided by the asymptotic analytical results and the numerical solutions, a simple yet accurate approximate analytical solution for the macroscopic viscoelastic response of the suspensions is proposed.

1. Introduction

In spite of its ever-increasing practical relevance in engineering technologies and biological systems alike, a fundamental problem in mechanics that so far has been sidestepped in the literature is that of the homogenization of nonlinear viscoelastic composite materials undergoing finite deformations. This avoidance is likely due to the three simultaneous technical challenges that the problem involves:

(i) Long-range memory. The first technical challenge has to do with the fact that even viscoelastic composite materials made of constituents featuring the simplest types of short-range-memory behaviors, after homogenization, turn out in general to feature

* Corresponding author.
E-mail addresses: kg5@illinois.edu (K. Ghosh), bshrima2@illinois.edu (B. Shrimali), akumar51@illinois.edu (A. Kumar), pamies@illinois.edu (O. Lopez-Pamies).

https://doi.org/10.1016/j.jmps.2021.104544
Received 4 March 2021; Received in revised form 13 May 2021; Accepted 14 June 2021
Available online 20 June 2021

long-range-memory behaviors.[1] This was first shown by Sanchez-Palencia (1980, Chapter 6) and Francfort and Suquet (1986) for linear viscoelastic composite materials with Kelvin–Voigt constituents, and by Suquet (1987, Chapter 3) for composite materials with Maxwell constituents.

(ii) Constitutive nonlinearity. The traverse of long-range memory can be convincingly handled with the Laplace transform and the correspondence principle when dealing with *linear* viscoelasticity; see, e.g., Hashin (1965, 1970), Yeong-Moo et al. (1998), Lahellec and Suquet (2007a), and Idiart et al. (2020). However, no such powerful tool exists to deal with constitutively *nonlinear* viscoelastic materials.

Nevertheless, by restricting attention to the asymptotic setting of infinitesimally small deformations and leveraging homogenization techniques developed for nonlinear elastic materials within that same asymptotic setting, progress has been made over the past twenty-five years in both numerical and analytical fronts. Indeed, numerical methods based on conventional finite elements (FE) and fast Fourier transforms (FFT) for the discretization of space together with a standard first-order implicit discretization in time have been successfully implemented to generate homogenization solutions not only for linear but also for a variety of nonlinear viscoelastic materials; see, e.g., Brinson and Knauss (1991), Lévesque et al. (2004), Lahellec and Suquet (2007c), and Pallicity and Böhlke (2021). Likewise, analytical methods based on the "linearization" of the nonlinear viscoelastic constituents have also been introduced to generate approximate solutions with reasonable success; see, e.g., Li and Weng (1997), Brenner et al. (2002), and Lahellec and Suquet (2007b).

(iii) Geometric nonlinearity. The third technical challenge is posed by the geometric nonlinearity inherent to finite deformations. Precisely, on the one hand, finite deformations imply that the elastic part of the constitutive behavior of viscoelastic materials is nonconvex. This poses significant problems for both numerical and analytical methods of solution; for numerical methods, for example, it is well-known that extreme care should be exercised in the selection of the time discretization when dealing with the nonconvex constraint of incompressibility (Simo, 1992). On the other hand, and perhaps more importantly, finite deformations imply as well that the microstructure of the composite material at hand evolves and hence that it must be tracked. This too poses significant difficulties for any method of solution. These are more acute for viscoelastic *fluids* than for viscoelastic *solids*. This is because the latter (Le Tallec et al., 1993; Reese and Govindjee, 1998; Kumar and Lopez-Pamies, 2016), as opposed to the former (Brady and Bossis, 1988; Hu, 1998), can be treated with a Lagrangian description of the kinematics, which allows to account implicitly for the evolution of microstructure.

In this context, this paper aims at providing a first[2] homogenization result in nonlinear finite viscoelasticity. Our interest is on suspensions of rigid inclusions in rubber. Within such a physically prominent class of materials, we restrict attention to the prototypical case of random isotropic suspensions of equiaxed inclusions — *id est*, inclusions that are roughly spherical in shape but that are not necessarily smooth or without a slightly preferred direction — that are firmly embedded in an isotropic incompressible Gaussian rubber with constant viscosity.

We begin in Section 2 by formulating the pertinent homogenization problem. Sections 3 through 5 are devoted to working out the solutions in several asymptotic limits for which the governing initial–boundary-value problem admits analytical treatment. These include the limit of small deformations (Section 3), the limit of finite deformations that are applied either infinitesimally slowly or "infinitely" fast (Section 4), and the limit when the underlying rubber matrix does not store elastic energy and degenerates into a Newtonian fluid (Section 5). Section 6 presents a numerical scheme to solve the governing initial–boundary-value problem under arbitrary finite deformations and loading conditions. The scheme makes use of a conforming Crouzeix–Raviart FE discretization of space and a high-order accurate explicit Runge–Kutta discretization of time. The combination of these two types of discretizations results into a robust scheme that is capable of handling finite deformations and the incompressibility constraint of the rubber for general loading conditions, irrespectively of whether they are applied slowly, fast, or span a large time range. In Section 7, we deploy the proposed scheme to generate sample solutions for the basic case of suspensions of spherical inclusions of the same (monodisperse) size under a variety of loading conditions suitably selected so as to extract the distinctive features of the macroscopic response of the suspensions. Guided by the asymptotic solutions in Sections 3 through 5 and the numerical solutions in Section 7, we propose in Section 8 a simple yet accurate approximate analytical solution for the macroscopic viscoelastic response of the suspensions. Most notably, consistent with the asymptotic and numerical solutions, the two distinguishing characteristics of this approximate solution are that it features the same type of short-range-memory behavior as that of the underlying rubber, with the caveat that its effective viscosity is *not* constant, as that of the rubber, but instead is a nonlinear viscosity of shear-thinning type. We close by recording a number of final comments in Section 9.

[1] By short-range-memory viscoelastic behaviors we mean viscoelastic behaviors that can be written in terms of a single internal variable, possibly tensorial, that is solution of a first-order ordinary differential equation (ODE) in time. On the other hand, by long-range-memory viscoelastic behaviors we mean viscoelastic behaviors that are described by hereditary integrals which cannot be reduced to a single first-order ODE. As an alternative terminology, short- and long-range-memory viscoelastic behaviors may also be referred to as narrow- and broad-spectrum behaviors.

[2] While no homogenization result in nonlinear finite viscoelasticity has yet been presented in the literature — at least, we are not aware of any — we should mention that strides have been made over the past two decades in advancing computational homogenization results in the related internal-variable-based context of finite crystal plasticity; see Miehe et al. (2002) and Roters et al. (2010), for example.

2. The problem

2.1. Microscopic description of the suspensions

Kinematics. Consider a random isotropic suspension of equiaxed, but of arbitrary shape otherwise, inclusions firmly embedded in an isotropic incompressible rubber matrix. In its initial configuration, presumed to be undeformed and stress-free, at time $t = 0$, the bounded domain in $\mathbb{R}^3$ occupied by any such two-phase composite material is denoted by Ω_0 and its boundary by $\partial\Omega_0$. The subdomains occupied by the rubber matrix ($\mathtt{m}$) and collectively by the inclusions ($\mathtt{i}$) are denoted by $\Omega_0^{(\mathtt{m})}$ and $\Omega_0^{(\mathtt{i})} = \Omega_0 \backslash \Omega_0^{(\mathtt{m})}$, respectively. The inclusions are taken to be of much smaller sizes than the macroscopic length scale of Ω_0.

Material points are identified by their initial position vector $\mathbf{X} \in \Omega_0$. At a later time $t \in (0, T]$, in response to externally applied mechanical stimuli to be described below, the position vector $\mathbf{X}$ of a material point moves to a new position specified by

$$\mathbf{x} = \mathbf{y}(\mathbf{X}, t),$$

where $\mathbf{y}$ is an invertible mapping from Ω_0 to the current configuration $\Omega(t)$, also contained in $\mathbb{R}^3$. We write the deformation gradient and Lagrangian velocity fields at $\mathbf{X}$ and t as

$$\mathbf{F}(\mathbf{X}, t) = \nabla \mathbf{y}(\mathbf{X}, t) = \frac{\partial \mathbf{y}}{\partial \mathbf{X}}(\mathbf{X}, t) \qquad \text{and} \qquad \mathbf{V}(\mathbf{X}, t) = \dot{\mathbf{y}}(\mathbf{X}, t) = \frac{\partial \mathbf{y}}{\partial t}(\mathbf{X}, t).$$

The "dot" notation will also be used throughout to denote the material time derivative (i.e., with $\mathbf{X}$ held fixed) of other field quantities.

Constitutive behavior of the rubber. Making use of the two-potential formalism (Halphen and Nguyen, 1975; Ziegler and Wehrli, 1987; Kumar and Lopez-Pamies, 2016), the isothermal constitutive behavior of the rubber is taken to be characterized by two thermodynamic potentials that describe how it stores energy through elastic deformation as well as how it dissipates energy through viscous deformation: (i) a free-energy function $\psi_{\mathtt{m}}$ and (ii) a dissipation potential $\phi_{\mathtt{m}}$.

The focus here is on the prototypical case of *Gaussian* rubber with *constant viscosity*, accordingly

$$\psi_{\mathtt{m}}(\mathbf{F}, \mathbf{F}^v) = \begin{cases} \underbrace{\frac{\mu_{\mathtt{m}}}{2}\left[I_1 - 3\right]}_{\psi_{\mathtt{m}}^{\mathrm{Eq}}(\mathbf{F})} + \underbrace{\frac{\nu_{\mathtt{m}}}{2}\left[I_1^e - 3\right]}_{\psi_{\mathtt{m}}^{\mathrm{NEq}}\left(\mathbf{F}\mathbf{F}^{v-1}\right)} & \text{if} \quad J = 1 \\ +\infty & \text{otherwise} \end{cases} \tag{1}$$

and

$$\phi_{\mathtt{m}}(\mathbf{F}, \mathbf{F}^v, \dot{\mathbf{F}}^v) = \begin{cases} \frac{1}{2}\dot{\mathbf{F}}^v\mathbf{F}^{v-1} \cdot \left[2\,\eta_{\mathtt{m}}\,\boldsymbol{\mathcal{K}}\,\dot{\mathbf{F}}^v\mathbf{F}^{v-1}\right] & \text{if} \quad \mathrm{tr}\left(\dot{\mathbf{F}}^v\mathbf{F}^{v-1}\right) = 0 \\ +\infty & \text{otherwise} \end{cases}. \tag{2}$$

In these expressions, the second-order tensor $\mathbf{F}^v$ is an internal variable of state that corresponds roughly to the "viscous part" of the deformation gradient[3] $\mathbf{F}$,

$$I_1 = \mathbf{F} \cdot \mathbf{F} = \mathrm{tr}\,\mathbf{C}, \quad J = \det \mathbf{F} = \sqrt{\det \mathbf{C}}, \quad I_1^e = \mathbf{F}\mathbf{F}^{v-1} \cdot \mathbf{F}\mathbf{F}^{v-1} = \mathrm{tr}\left(\mathbf{C}\mathbf{C}^{v-1}\right),$$

where $\mathbf{C} = \mathbf{F}^T\mathbf{F}$ denotes the right Cauchy–Green deformation tensor, $\mathbf{C}^v = \mathbf{F}^{vT}\mathbf{F}^v$,

$$\mathcal{K}_{ijkl} = \frac{1}{2}\left(\delta_{ik}\delta_{jl} + \delta_{il}\delta_{jk} - \frac{2}{3}\delta_{ij}\delta_{kl}\right) \tag{3}$$

stands for the standard deviatoric orthogonal projection tensor, and $\mu_{\mathtt{m}} \geq 0$, $\nu_{\mathtt{m}} \geq 0$, $\eta_{\mathtt{m}} \geq 0$ are material constants; the units of $\mu_{\mathtt{m}}$ and $\nu_{\mathtt{m}}$ are $force/length^2$, while $\eta_{\mathtt{m}}$ has units of $force \times time/length^2$.

The interested reader is referred to Kumar and Lopez-Pamies (2016) for a complete description of the two-potential framework as it pertains to rubber. Here, it suffices to recall that, from a theoretical point of view, the thermodynamic potentials (1)–(2) satisfy the principle of material frame indifference (or objectivity), the material symmetry requirements of isotropy, and the reduced dissipation inequality, while, from a practical point of view, they capture the five basic features of rubber viscoelasticity, to wit:

- the storage of energy is primarily governed by changes in entropy of the underlying polymer network,
- the dissipation of energy is primarily governed by friction among neighboring polymer chains,
- when all forces are removed after an arbitrary loading path, rubber creeps back to its original configuration,
- when subjected to relaxation and creep loading conditions, rubber exhibits a transient response that then evolves into an equilibrium state of deformation and stress, and

[3] More specifically, the internal variable $\mathbf{F}^v$ is such that $\mathbf{F} = \mathbf{F}^e\mathbf{F}^v$, where $\mathbf{F}^e$ corresponds roughly to the "elastic part" of the deformation gradient tensor $\mathbf{F}$. In the context of finite viscoelasticity, such a multiplicative type of internal variable appears to have been first put forth by Sidoroff (1974). Other *constitutive* definitions — for instance, one where $\mathbf{F} = \mathbf{F}^v\mathbf{F}^e$ — are of course possible for the internal variable $\mathbf{F}^v$. The one utilized here is not only amply general but also the most common in the literature.

- when subjected to loading conditions of the same type but different loading rate, rubber exhibits different responses.

Specifically, the function $\psi_{\mathtt{m}}^{\mathrm{Eq}}$ in (1) characterizes the elastic energy storage in the rubber at states of thermodynamic equilibrium, whereas $\psi_{\mathtt{m}}^{\mathrm{NEq}}$ characterizes the additional elastic energy storage at non-equilibrium states (i.e., the part of the energy that gets dissipated eventually). Accordingly, $\psi_{\mathtt{m}}^{\mathrm{Eq}}$ is a function solely of the deformation gradient $\mathbf{F}$, while $\psi_{\mathtt{m}}^{\mathrm{NEq}}$ depends on $\mathbf{F}$ and additionally on the internal variable $\mathbf{F}^{v}$. On the other hand, the constant $\eta_{\mathtt{m}}$ in (2) characterizes the viscosity of the rubber. By now it is well-established from statistical mechanics (Treloar, 1975; Doi and Edwards, 1998), and more so from an abundance of macroscopic experimental results, that at sufficiently large deformations and deformation rates the elasticity of rubber is non-Gaussian and that its viscosity is nonlinear. We shall comment further on these additional nonlinearities in Section 9 below.

In the spirit of the classical linear theory of viscoelasticity (Gross, 1953), it proves instructive to visualize the physical meaning of the two thermodynamic potentials (1)–(2) pictorially in the form of a rheological model. Fig. 1 provides such a representation, which can be readily identified as the classical Zener — or standard solid — model for viscoelastic solids (Zener, 1948) generalized to account for the constitutive and geometric nonlinearities inherent to finite deformations.

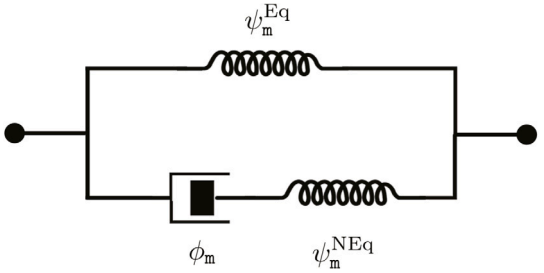

Fig. 1. Rheological model of rubber.

Constitutive behavior of the inclusions. The rigid behavior of the inclusions can also be conveniently cast within the two-potential formalism. In this case, the free-energy function can be simply written as

$$\psi_{\mathtt{i}}(\mathbf{F}) = \begin{cases} 0 & \text{if} \quad \mathbf{F} = \mathbf{Q} \in Orth^{+} \\ +\infty & \text{otherwise} \end{cases}, \tag{4}$$

where $Orth^{+}$ stands for the set of all proper orthogonal second-order tensors, while the dissipation potential is identically 0.

In order to account for the perfectly rigid behavior (4) within the context of the numerical scheme introduced below in Section 6, it will prove expedient not to work with (4) directly but to consider instead the regularized and hence more general case of elastic isotropic inclusions with free-energy function

$$\psi_{\mathtt{i}}(\mathbf{F}) = \frac{\mu_{\mathtt{i}}}{2}\left[I_1 - 3\right] - \mu_{\mathtt{i}} \ln J, \tag{5}$$

where the parameter $\mu_{\mathtt{i}}$ denotes the shear modulus of the inclusions in their undeformed state; by the same token, their bulk modulus is given by $\kappa_{\mathtt{i}} = \frac{2}{3}\mu_{\mathtt{i}}$. The perfectly rigid behavior (4) can then be readily recovered as a special case of (5) by taking the limit of $\mu_{\mathtt{i}} \to +\infty$.

Pointwise constitutive behavior of the suspension. Given the free-energy functions (1), (5), and the dissipation potential (2), it follows that the first Piola–Kirchhoff stress tensor $\mathbf{S}$ at any material point $\mathbf{X} \in \Omega_0$ and time $t \in [0, T]$ is expediently given by the relation (Kumar and Lopez-Pamies, 2016)

$$\mathbf{S}(\mathbf{X}, t) = \frac{\partial \psi}{\partial \mathbf{F}}(\mathbf{X}, \mathbf{F}, \mathbf{F}^{v}), \tag{6}$$

where $\mathbf{F}^{v}$ is implicitly defined by the evolution equation

$$\begin{cases} \dfrac{\partial \psi}{\partial \mathbf{F}^{v}}(\mathbf{X}, \mathbf{F}, \mathbf{F}^{v}) + \dfrac{\partial \phi}{\partial \dot{\mathbf{F}}^{v}}(\mathbf{X}, \mathbf{F}, \mathbf{F}^{v}, \dot{\mathbf{F}}^{v}) = \mathbf{0} \\ \mathbf{F}^{v}(\mathbf{X}, 0) = \mathbf{I} \end{cases}, \tag{7}$$

and where

$$\psi(\mathbf{X}, \mathbf{F}, \mathbf{F}^{v}) = \left(1 - \theta_{\mathtt{i}}(\mathbf{X})\right)\psi_{\mathtt{m}}(\mathbf{F}, \mathbf{F}^{v}) + \theta_{\mathtt{i}}(\mathbf{X})\psi_{\mathtt{i}}(\mathbf{F}) \quad \text{and} \quad \phi(\mathbf{X}, \mathbf{F}, \mathbf{F}^{v}, \dot{\mathbf{F}}^{v}) = \left(1 - \theta_{\mathtt{i}}(\mathbf{X})\right)\phi_{\mathtt{m}}(\mathbf{F}, \mathbf{F}^{v}, \dot{\mathbf{F}}^{v}).$$

In these relations, $\theta_{\mathtt{i}}$ denotes the characteristic function describing the spatial locations occupied by the inclusions in Ω_0, that is, $\theta_{\mathtt{i}}$ takes the value of 1 if $\mathbf{X} \in \Omega_0^{(\mathtt{i})}$ and 0 otherwise. For later use, we introduce the notation

$$c := \frac{1}{|\Omega_0|}\int_{\Omega_0} \theta_{\mathtt{i}}(\mathbf{X})\mathrm{d}\mathbf{X} = \frac{|\Omega_0^{(\mathtt{i})}|}{|\Omega_0|}$$

for the volume fraction of inclusions in the suspension.

Upon direct use of the potentials (1), (2), (5), together with some algebraic manipulation, the pointwise constitutive response (6)–(7) of the suspension takes the more explicit form

$$\mathbf{S}(\mathbf{X},t)=\left(1-\theta_{\mathrm{i}}(\mathbf{X})\right)\left(\mu_{\mathrm{m}}\mathbf{F}-p\mathbf{F}^{-T}+\nu_{\mathrm{m}}\mathbf{F}\mathbf{C}^{v-1}\right)+\theta_{\mathrm{i}}(\mathbf{X})\mu_{\mathrm{i}}\left(\mathbf{F}-\mathbf{F}^{-T}\right), \tag{8}$$

where p stands for the arbitrary hydrostatic pressure associated with the incompressibility constraint $J=1$ of the rubber and $\mathbf{C}^v$ is defined by the evolution equation

$$\begin{cases}\dot{\mathbf{C}}^v(\mathbf{X},t)=\dfrac{\nu_{\mathrm{m}}}{\eta_{\mathrm{m}}}\left[\mathbf{C}-\dfrac{1}{3}\left(\mathbf{C}\cdot\mathbf{C}^{v-1}\right)\mathbf{C}^v\right]\\ \mathbf{C}^v(\mathbf{X},0)=\mathbf{I}\end{cases}. \tag{9}$$

Note that the dependence on the internal variable $\mathbf{F}^v$ enters (8) and (9) only through the symmetric combination $\mathbf{C}^v=\mathbf{F}^{vT}\mathbf{F}^v$.

2.2. Macroscopic or homogenized response

In light of the assumed small size of the inclusions and of their isotropic and hence statistically uniform spatial distribution, the microscopically heterogeneous suspension described above is expected to behave macroscopically as a homogeneous material. Its macroscopic or homogenized response can be defined as the relation between the history of the volume average of the first Piola–Kirchhoff stress

$$\{\mathbf{S}(t),\ t\in[0,T]\},\qquad \mathbf{S}(t):=\frac{1}{|\Omega_0|}\int_{\Omega_0}\mathbf{S}(\mathbf{X},t)\,\mathrm{d}\mathbf{X} \tag{10}$$

and the history of the volume average of the deformation gradient

$$\{\mathbf{F}(t),\ t\in[0,T]\},\qquad \mathbf{F}(t):=\frac{1}{|\Omega_0|}\int_{\Omega_0}\mathbf{F}(\mathbf{X},t)\,\mathrm{d}\mathbf{X} \tag{11}$$

when it is subjected to affine boundary conditions (Hill, 1972; Suquet, 1987).

Restricting attention, for definiteness, to affine deformations when $\mathbf{F}(t)$ is prescribed, the problem amounts to solving the initial–boundary-value problem

$$\begin{cases}\mathrm{Div}\left[\left(1-\theta_{\mathrm{i}}(\mathbf{X})\right)\left(\mu_{\mathrm{m}}\nabla\mathbf{y}-p\nabla\mathbf{y}^{-T}+\nu_{\mathrm{m}}\nabla\mathbf{y}\mathbf{C}^{v-1}\right)+\theta_{\mathrm{i}}(\mathbf{X})\mu_{\mathrm{i}}\left(\nabla\mathbf{y}-\nabla\mathbf{y}^{-T}\right)\right]=\mathbf{0}, & (\mathbf{X},t)\in\Omega_0\times[0,T]\\ \det\nabla\mathbf{y}=1, & (\mathbf{X},t)\in\Omega_0^{(\mathrm{m})}\times[0,T]\\ \mathbf{y}(\mathbf{X},t)=\mathbf{F}(t)\mathbf{X}, & (\mathbf{X},t)\in\partial\Omega_0\times[0,T]\\ \mathbf{y}(\mathbf{X},0)=\mathbf{X}, & \mathbf{X}\in\Omega_0\end{cases} \tag{12}$$

coupled with the evolution equation

$$\begin{cases}\dot{\mathbf{C}}^v(\mathbf{X},t)=\dfrac{\nu_{\mathrm{m}}}{\eta_{\mathrm{m}}}\left[\nabla\mathbf{y}^T\nabla\mathbf{y}-\dfrac{1}{3}\left(\nabla\mathbf{y}^T\nabla\mathbf{y}\cdot\mathbf{C}^{v-1}\right)\mathbf{C}^v\right], & (\mathbf{X},t)\in\Omega_0^{(\mathrm{m})}\times[0,T]\\ \mathbf{C}^v(\mathbf{X},0)=\mathbf{I}, & \mathbf{X}\in\Omega_0^{(\mathrm{m})}\end{cases} \tag{13}$$

for the deformation field $\mathbf{y}(\mathbf{X},t)$, the pressure field $p(\mathbf{X},t)$, and the internal variable $\mathbf{C}^v(\mathbf{X},t)$ for the case when $\mu_{\mathrm{i}}=+\infty$, and then computing the resulting history of the macroscopic stress (10).

Eq. $(12)_1$ is nothing more than balance of linear momentum in the absence of inertia and body forces, $\mathrm{Div}\,\mathbf{S}=\mathbf{0}$, specialized to the constitutive behavior (8). Balance of angular momentum, $\mathbf{S}\mathbf{F}^T=\mathbf{F}\mathbf{S}^T$, is automatically satisfied by virtue of the material frame indifference of the free-energy functions (1) and (5) and of the dissipation potential (2); see Section 2.1 in Kumar and Lopez-Pamies (2016).

In general, the nonlinear initial–boundary-value problem (12)–(13) can only be solved numerically by means of schemes that discretize both space and time. As announced in the Introduction, one of the main objectives of this work is to put forth one such scheme alongside sample numerical solutions for the history of the macroscopic stress (10) in terms of the history of the macroscopic deformation gradient (11) aimed at extracting the distinctive features of the macroscopic response of the suspension. We do so in Sections 6 and 7. As elaborated prior to that in Sections 3, 4, and 5, nevertheless, Eqs. (12)–(13) permit great simplification in several basic limits of physical significance. Those are the limits of: (*i*) small deformations, (*ii*) finite deformations for slow and fast deformation rates, and (*iii*) finite deformations in the absence of storage of elastic energy when the rubber reduces to a Newtonian fluid. The second main objective of this work is to put forth a simple approximate solution for the macroscopic constitutive relation between (10) and (11) for arbitrary finite deformations and loading conditions. This, again, we do in Section 8 with direct guidance from the asymptotically exact and computational solutions worked out in Sections 3 through 7.

3. The homogenized response in the small-deformation limit

In the limit of small deformations as $\|\mathbf{F}(t)-\mathbf{I}\|\to 0$, the nonlinear viscoelasticity problem (12)–(13) reduces asymptotically to one of linear viscoelasticity that can be solved exactly — by virtue of the incompressibility of the rubber matrix and rigidity

of the inclusions — in terms of a *single linear elastostatics* problem by means of the correspondence principle. It follows that the macroscopic constitutive response of the suspension in such a limit, as characterized by the relation between the histories of their macroscopic stress (10) and macroscopic deformation gradient (11), can be written in closed form in terms of the solution of the pertinent elastostatics problem. The derivation of this asymptotic result goes as follows.

Introduce the macroscopic deformation measure $\mathsf{H}(t) = \mathsf{F}(t) - \mathbf{I}$ and consider solutions to (12)–(13) of the asymptotic form

$$\begin{aligned}
&\mathbf{y}(\mathbf{X},t) = \mathbf{X} + \mathbf{u}(\mathbf{X},t) + O(\|\mathsf{H}(t)\|^2) \qquad \text{with} \qquad u_i(\mathbf{X},t) = \Gamma_{ijk}(\mathbf{X},t)\mathsf{H}_{jk}(t),\\
&p(\mathbf{X},t) = \mu_{\mathrm{m}} + \nu_{\mathrm{m}} + p_0(\mathbf{X},t) + O(\|\mathsf{H}(t)\|^2) \qquad \text{with} \qquad p_0(\mathbf{X},t) = \Sigma_{jk}(\mathbf{X},t)\mathsf{H}_{jk}(t),\\
&\mathbf{C}^v(\mathbf{X},t) = \mathbf{I} + \mathbf{H}^v(\mathbf{X},t) + \mathbf{H}^{vT}(\mathbf{X},t) + O(\|\mathsf{H}(t)\|^2) \qquad \text{with} \qquad H^v_{ij}(\mathbf{X},t) = Y_{ijkl}(\mathbf{X},t)\mathsf{H}_{kl}(t)
\end{aligned}$$

in the limit as $\|\mathsf{H}(t)\| \to 0$; the tensors $\boldsymbol{\Gamma}$, $\boldsymbol{\Sigma}$, $\boldsymbol{Y}$ quantifying the linearity of the fields in $\mathsf{H}(t)$ are commonly referred to as "concentration" tensors. By making explicit use of this ansatz, standard calculations show that the Eqs. (12)–(13) reduce to $O(\|\mathsf{H}(t)\|)$ to the initial–boundary-value problem

$$\begin{cases}
\operatorname{Div}\left[\left(1-\theta_{\mathrm{i}}(\mathbf{X})\right)\left(\mu_{\mathrm{m}}(\nabla\mathbf{u}+\nabla\mathbf{u}^T) - p_0\mathbf{I} + \nu_{\mathrm{m}}\left(\nabla\mathbf{u}+\nabla\mathbf{u}^T - \mathbf{H}^v - \mathbf{H}^{vT}\right)\right) + \right.\\
\qquad \left. \theta_{\mathrm{i}}(\mathbf{X})\mu_{\mathrm{i}}\left(\nabla\mathbf{u}+\nabla\mathbf{u}^T\right)\right] = \mathbf{0}, & (\mathbf{X},t) \in \Omega_0 \times [0,T]\\
\operatorname{tr}\nabla\mathbf{u} = 0, & (\mathbf{X},t) \in \Omega_0^{(\mathrm{m})} \times [0,T]\\
\mathbf{u}(\mathbf{X},t) = \mathsf{H}(t)\mathbf{X}, & (\mathbf{X},t) \in \partial\Omega_0 \times [0,T]\\
\mathbf{u}(\mathbf{X},0) = \mathbf{0}, & \mathbf{X} \in \Omega_0
\end{cases} \tag{14}$$

coupled with the evolution equation

$$\begin{cases}
\dot{\mathbf{H}}^v(\mathbf{X},t) = \dfrac{\nu_{\mathrm{m}}}{\eta_{\mathrm{m}}}\left[\nabla\mathbf{u} - \mathbf{H}^v\right], & (\mathbf{X},t) \in \Omega_0^{(\mathrm{m})} \times [0,T]\\
\mathbf{H}^v(\mathbf{X},0) = \mathbf{0}, & \mathbf{X} \in \Omega_0^{(\mathrm{m})}
\end{cases} \tag{15}$$

for the displacement field $\mathbf{u}(\mathbf{X},t)$, the pressure field $p_0(\mathbf{X},t)$, and the internal variable $\mathbf{H}^v(\mathbf{X},t)$.

Upon recognizing that the linear system of ODEs (15) admits the simple explicit solution

$$\mathbf{H}^v(\mathbf{X},t) = \int_0^t \frac{e^{-\frac{t-\tau}{\tau_{\mathrm{m}}}}}{\tau_{\mathrm{m}}} \nabla\mathbf{u}(\mathbf{X},\tau)\mathrm{d}\tau, \qquad \tau_{\mathrm{m}} := \frac{\eta_{\mathrm{m}}}{\nu_{\mathrm{m}}}, \tag{16}$$

and introducing the notation

$$\mathbf{L}(\mathbf{X},t) = \left(1-\theta_{\mathrm{i}}(\mathbf{X})\right)\mathbf{L}_{\mathrm{m}}(t) + \theta_{\mathrm{i}}(\mathbf{X})\mathbf{L}_{\mathrm{i}} \qquad \text{with} \qquad \mathbf{L}_{\mathrm{m}}(t) = 2\left(\mu_{\mathrm{m}} + \nu_{\mathrm{m}}e^{-\frac{t}{\tau_{\mathrm{m}}}}\right)\boldsymbol{\mathcal{K}} \qquad \text{and} \qquad \mathbf{L}_{\mathrm{i}} = 2\mu_{\mathrm{i}}\boldsymbol{\mathcal{I}}$$

for the initial relaxation function of the suspension, the Eqs. (14)–(15) can be recast in the more compact form

$$\begin{cases}
\operatorname{Div}\left[\displaystyle\int_{-\infty}^{t} \mathbf{L}(\mathbf{X},t-\tau)\frac{\partial\nabla\mathbf{u}}{\partial\tau}(\mathbf{X},\tau)\mathrm{d}\tau - (1-\theta_{\mathrm{i}}(\mathbf{X}))p_0\mathbf{I}\right] = \mathbf{0}, & (\mathbf{X},t) \in \Omega_0 \times [0,T]\\
\operatorname{tr}\nabla\mathbf{u} = 0, & (\mathbf{X},t) \in \Omega_0^{(\mathrm{m})} \times [0,T]\\
\mathbf{u}(\mathbf{X},t) = \mathsf{H}(t)\mathbf{X}, & (\mathbf{X},t) \in \partial\Omega_0 \times [0,T]\\
\mathbf{u}(\mathbf{X},0) = \mathbf{0}, & \mathbf{X} \in \Omega_0
\end{cases} . \tag{17}$$

In these last expressions, $\boldsymbol{\mathcal{K}}$ stands, again, for the deviatoric orthogonal projection tensor (3), $\mathcal{I}_{ijkl} = \frac{1}{2}(\delta_{ik}\delta_{jl} + \delta_{il}\delta_{jk})$ denotes the identity in the space of fourth-order tensors with major and minor symmetries, and it is tacitly assumed that $\mathbf{u}(\mathbf{X},t) = \mathbf{0}$ for $t < 0$.

Next, define the one-sided Laplace transform of any function of time $f(t)$ in the usual manner as

$$\mathcal{L}\{f(t)\} = \widehat{f}(s) = \int_0^\infty f(t)e^{-st}\,\mathrm{d}t.$$

Applying this transform to Eqs. (17) leads to

$$\begin{cases}
\operatorname{Div}\left[\widetilde{\mathbf{L}}(\mathbf{X},s)\nabla\widehat{\mathbf{u}}(\mathbf{X},s) - (1-\theta_{\mathrm{i}}(\mathbf{X}))\widehat{p}_0\mathbf{I}\right] = \mathbf{0}, & \mathbf{X} \in \Omega_0\\
\operatorname{tr}\nabla\widehat{\mathbf{u}} = 0, & \mathbf{X} \in \Omega_0^{(\mathrm{m})}\\
\widehat{\mathbf{u}}(\mathbf{X},s) = \widehat{\mathbf{H}}(s)\mathbf{X}, & \mathbf{X} \in \partial\Omega_0\\
\widehat{\mathbf{u}}(\mathbf{X},0) = \mathbf{0}, & \mathbf{X} \in \Omega_0
\end{cases} , \tag{18}$$

where

$$\widetilde{\mathbf{L}}(\mathbf{X},s) = s\widehat{\mathbf{L}}(\mathbf{X},s) = \left(1-\theta_{\mathrm{i}}(\mathbf{X})\right)s\widehat{\mathbf{L}}_{\mathrm{m}}(s) + \theta_{\mathrm{i}}(\mathbf{X})\mathbf{L}_{\mathrm{i}} = \left(1-\theta_{\mathrm{i}}(\mathbf{X})\right)2\left(\mu_{\mathrm{m}} + \frac{\nu_{\mathrm{m}}\tau_{\mathrm{m}}s}{1+\tau_{\mathrm{m}}s}\right)\boldsymbol{\mathcal{K}} + \theta_{\mathrm{i}}(\mathbf{X})2\mu_{\mathrm{i}}\boldsymbol{\mathcal{I}}.$$

As expected, the governing Eqs. (18) in the Laplace domain for the fields $\widehat{\mathbf{u}}(\mathbf{X}, s)$ and $\widehat{p}_0(\mathbf{X}, s)$ feature identical mathematical structure as the governing equations for the displacement and pressure fields in a linear elastic composite material with the same two-phase particulate microstructure as the viscoelastic suspension — the "only" difference is that the constitutive properties and boundary conditions in (18) are parameterized by the Laplace variable s. Accordingly, the same standard techniques of solution employed for linear elastostatics problems apply to (18) directly. Once computed, however, the solution needs to be transformed back to the time domain, which, in principle, can take considerable effort; see, e.g., Yeong-Moo et al. (1998).

Now, for the case of the isotropic suspension of *rigid* inclusions embedded in an isotropic *incompressible* matrix of interest here, it so happens that the dependence on the Laplace variable s can be factored out of the equilibrium equation (18); we discuss how this remarkable feature applies to much more general viscoelastic composite materials — not just two-phase particulate composite materials with isotropic incompressible matrix and rigid inclusions — in Section 9 below. It follows that the displacement and pressure fields solution of (18) are then of the simple separable form

$$\widehat{u}_i(\mathbf{X}, s) = \varGamma_{ikl}(\mathbf{X})\widehat{\mathrm{H}}_{kl}(s) \qquad \text{and} \qquad \widehat{p}_0(\mathbf{X}, s) = \varSigma_{ij}(\mathbf{X})\widehat{\mathrm{H}}_{ij}(s), \tag{19}$$

where the concentration tensors $\boldsymbol{\varGamma}(\mathbf{X})$ and $\boldsymbol{\varSigma}(\mathbf{X})$ are solution of the *s-independent* linear elastostatics problem[4]

$$\begin{cases} \dfrac{\partial}{\partial X_j}\left[\left(1-\theta_{\mathrm{i}}(\mathbf{X})+k\theta_{\mathrm{i}}(\mathbf{X})\right)\boldsymbol{\mathcal{K}}_{ijmn}\dfrac{\partial \varGamma_{mkl}}{\partial X_n}(\mathbf{X})+\delta_{ij}\varSigma_{kl}(\mathbf{X})\right]=0, & \mathbf{X}\in\varOmega_0 \\ \dfrac{\partial \varGamma_{mkl}}{\partial X_m}(\mathbf{X})=0, & \mathbf{X}\in\varOmega_0 \\ \varGamma_{ikl}(\mathbf{X})=\delta_{ik}X_l, & \mathbf{X}\in\partial\varOmega_0 \end{cases}, \quad \text{with} \quad k=+\infty. \tag{20}$$

Granted the separable solution (19), the otherwise intensive passage from the Laplace domain to the time domain is trivial in this case. By the same token, the computation of the history of the macroscopic stress (10) is straightforward. It reads

$$\mathbf{S}(t) = \overline{\mu}\left(\mathbf{H}+\mathbf{H}^T\right) - p\,\mathbf{I} + \overline{\nu}\left(\mathbf{H}+\mathbf{H}^T-\mathbf{H}^v-\mathbf{H}^{vT}\right) + O\left(\|\mathbf{H}\|^2\right), \tag{21}$$

where p stands for the arbitrary hydrostatic pressure associated with the incompressibility constraint $\mathrm{tr}\,\mathbf{H}=0$, $\mathbf{H}^v$ is defined by the evolution equation

$$\begin{cases} \dot{\mathbf{H}}^v(t) = \dfrac{\overline{\nu}}{\overline{\eta}}\left[\mathbf{H}-\mathbf{H}^v\right] \\ \mathbf{H}^v(0)=\mathbf{0} \end{cases}, \tag{22}$$

and where the three effective material constants $\overline{\mu}$, $\overline{\nu}$, $\overline{\eta}$ are given by the expressions

$$\overline{\mu} = g(c)\mu_{\mathrm{m}}, \qquad \overline{\nu} = g(c)\nu_{\mathrm{m}}, \qquad \overline{\eta} = g(c)\eta_{\mathrm{m}} \tag{23}$$

in terms of the enhancement coefficient

$$g(c) = \frac{1}{5|\varOmega_0|}\int_{\varOmega_0}\left(1-\theta_{\mathrm{i}}(\mathbf{X})+k\theta_{\mathrm{i}}(\mathbf{X})\right)\boldsymbol{\mathcal{K}}_{klmn}\frac{\partial \varGamma_{mkl}}{\partial X_n}(\mathbf{X})\mathrm{d}\mathbf{X}. \tag{24}$$

Remark 1. The enhancement coefficient (24) depends not only on the volume fraction c of the inclusions, but also on the specifics of their shape, relative size, and spatial distribution, as characterized by the particular characteristic function θ_{i} of the suspension at hand. We use c as its only argument for notational simplicity. Its computation requires the solution of the boundary-value problem (20) for the concentration tensor $\boldsymbol{\varGamma}(\mathbf{X})$. In general, this problem does not admit analytical solutions, but it is fairly straightforward to generate numerical solutions for it by means of the FE method; see, e.g., the Appendix in Spinelli et al. (2015). This traverse notwithstanding, there are classes of suspensions of practical interest that do admit analytical solutions for (24). One such class is that generated by iterated homogenization (Norris, 1985; Avellaneda, 1987; Lefèvre and Lopez-Pamies, 2021). Within this class, for later use, we recall that the simplest solution for (24) is given by

$$g(c) = (1-c)^{-5/2}, \tag{25}$$

which is a generalization of the classical dilute solution of Einstein (1906) worked out separately by Brinkman (1952) and Roscoe (1952). It corresponds to a suspension of spherical inclusions of infinitely many sizes distributed in a manner such that they can fill the entire space, thus its percolation at $c=1$. Recent numerical solutions (Lopez-Pamies et al., 2013b; Lefèvre and Lopez-Pamies, 2017a) have shown that the result (25) is accurately descriptive of suspensions of equiaxed inclusions of the same or different sizes for volume fractions in the small-to-moderate range $c\in[0, 0.25]$. That is, the enhancement coefficient (24) is fairly insensitive to the shape, relative size, and spatial distribution of the inclusions up to about $c=0.25$.

[4] Note that the rigidity of the inclusions, $k=+\infty$, in these equations is purely formal. A proper treatment alongside its numerical implementation can be found in the work of Chi et al. (2016). Alternatively, for practical purposes, one may also set $k\geq 10^3$ and use Eq. (20) directly.

Remark 2. To leading $O(\|\mathbf{H}(t)\|)$, consistent with an observation due to Hashin (1965) for linear viscoelastic composites with infinite contrast, the macroscopic response (21)–(22) of the suspension is of identical functional form as the response of the underlying rubber matrix, namely, an isotropic incompressible Zener viscoelastic solid. Its three effective material constants (23) are simply those of the underlying rubber matrix multiplied by the very same enhancement coefficient (24), which necessarily coincides with the enhancement coefficient that emerges in the limiting case when the rubber matrix is linear elastic; see, e.g., Section 2.1 in Lefèvre and Lopez-Pamies (2017a).

In general, as already stressed in the Introduction, the homogenized response of viscoelastic composites is expected to exhibit a much more complicated time dependence than that of its constituents, even when these are of very simple type. The reason why the homogenized response (21)–(22) for suspensions of rigid inclusions in rubber is — contrary to the general expectation — of the same form as that of the underlying rubber matrix can be attributed to the fact that there is *only one* relaxation mechanism in the suspensions, namely, the shear relaxation of the rubber. We elaborate further on this key point in Section 9 below.

4. The homogenized response at finite deformations for slow and fast deformation rates

For the limiting cases of finite deformations that are applied either infinitesimally slowly or "infinitely" fast[5] in time t, the nonlinear viscoelasticity problem (12)–(13) reduces asymptotically — as one can surmise from the rheological model in Fig. 1 — to two *finite elastostatics* problems that are amenable to available methods of solution. We spell out the two relevant finite elastostatics problems alongside their solution next, one at a time.

4.1. The limiting case of infinitesimally slow deformations

Consider macroscopic deformation gradients $\mathbf{F}(t)$ that are applied slowly in time and that, without loss of generality, feature the asymptotic behavior

$$\mathbf{F}(t) = \mathbf{F}_0 + t^{-1}\mathbf{F}_1 + O(t^{-2}) \tag{26}$$

in the limit as $t \to T = +\infty$, where $\mathbf{F}_0$ and $\mathbf{F}_1$ stand for two (suitably well-behaved) constant second-order tensors of choice. Physically, the prescription (26) describes a macroscopic deformation gradient $\mathbf{F}_0$ that is applied infinitesimally slowly.

In view of (26), we look for solutions to (12)–(13) of the asymptotic form

$$\begin{aligned}
&\mathbf{y}(\mathbf{X},t) = \mathbf{y}_0(\mathbf{X}) + t^{-1}\mathbf{y}_1(\mathbf{X}) + O(t^{-2}),\\
&p(\mathbf{X},t) = p_0(\mathbf{X}) + t^{-1}p_1(\mathbf{X}) + O(t^{-2}),\\
&\mathbf{C}^v(\mathbf{X},t) = \mathbf{C}^v_0(\mathbf{X}) + t^{-1}\mathbf{C}^v_1(\mathbf{X}) + O(t^{-2})
\end{aligned} \tag{27}$$

in the limit as $t \to +\infty$. Recognizing from $(27)_3$ that

$$\dot{\mathbf{C}}^v = -t^{-2}\mathbf{C}^v_1 + O(t^{-3}) \qquad \text{and} \qquad \mathbf{C}^{v-1} = \mathbf{C}^{v-1}_0 - t^{-1}\mathbf{C}^{v-1}_0\mathbf{C}^v_1\mathbf{C}^{v-1}_0 + O(t^{-2}),$$

it is straightforward to solve equation (13) for the internal variable $\mathbf{C}^v(\mathbf{X},t)$ to leading order to determine that

$$\mathbf{C}^v_0 = \nabla\mathbf{y}_0^T\nabla\mathbf{y}_0.$$

In turn, it is straightforward to deduce that, to leading order, Eqs. (12) simplify to the boundary-value problem

$$\begin{cases}
\mathrm{Div}\left[\left(1-\theta_{\mathrm{i}}(\mathbf{X})\right)\left(\mu_{\mathrm{m}}\nabla\mathbf{y}_0 - (p_0-\nu_{\mathrm{m}})\nabla\mathbf{y}_0^{-T}\right) + \theta_{\mathrm{i}}(\mathbf{X})\mu_{\mathrm{i}}\left(\nabla\mathbf{y}_0 - \nabla\mathbf{y}_0^{-T}\right)\right] = \mathbf{0}, & \mathbf{X}\in\Omega_0\\
\det\nabla\mathbf{y}_0 = 1, & \mathbf{X}\in\Omega_0^{(\mathrm{m})}\\
\mathbf{y}_0(\mathbf{X}) = \mathbf{F}_0\mathbf{X}, & \mathbf{X}\in\partial\Omega_0
\end{cases} \tag{28}$$

for the deformation field $\mathbf{y}_0(\mathbf{X})$ and pressure field $p_0(\mathbf{X})$.

For the case of interest here when $\mu_{\mathrm{i}} = +\infty$, Eqs. (28) are nothing more than the governing equations for the homogenized elastic response of a random isotropic suspension of rigid inclusions, with characteristic function θ_{i}, embedded in a Gaussian rubber matrix with initial shear modulus μ_{m}. In a string of recent contributions, Lopez-Pamies et al. (2013a,b), Goudarzi et al. (2015), Lefèvre and Lopez-Pamies (2017a,b), and Lefèvre et al. (2019) have worked out rigorous computational and analytical results that include as a special case the solution for the homogenization problem (28) for a wide spectrum of characteristic functions θ_{i}. These works have also put forth a simple yet accurate approximate solution, which states that the homogenized elastic response of isotropic composites made of any number of different Gaussian rubber phases is itself Gaussian; see Section 6 in Lefèvre and Lopez-Pamies (2017a). Accordingly, when specialized to the suspensions of interest here, this approximate solution states that, in terms of the applied macroscopic deformation gradients (26), the macroscopic stress (10) is simply given by

$$\mathbf{S}(t) = \overline{\mu}\,\mathbf{F}_0 - p\,\mathbf{F}_0^{-T} + O(t^{-1}), \tag{29}$$

where we recall that the effective material constant $\overline{\mu}$ is given by expression $(23)_1$ and p stands for the arbitrary hydrostatic pressure associated with the incompressibility constraint $\det\mathbf{F}_0 = 1$ of the suspension.

[5] Since inertia is not taken into account, "infinitely" fast should be understood in the usual sense of loading conditions that are applied in a time scale that is much smaller than the characteristic relaxation time of the problem, in the present context $\tau_{\mathrm{m}} = \eta_{\mathrm{m}}/\nu_{\mathrm{m}}$, but still large enough that inertial effects can be neglected.

4.2. The limiting case of "infinitely" fast deformations

Consider now applied macroscopic deformation gradients $\mathbf{F}(t)$ of the form

$$\mathbf{F}(t) = \mathbf{I} + \mathcal{H}(t)\left(\mathbf{F}_0 - \mathbf{I}\right), \tag{30}$$

where $\mathcal{H}(t)$ stands for the Heaviside function

$$\mathcal{H}(t) = \begin{cases} 0 & \text{if } t \leq 0 \\ 1 & \text{if } t > 0 \end{cases} \tag{31}$$

and $\mathbf{F}_0$ is a (suitably well-behaved) constant second-order tensor of choice. Physically, the prescription (30) describes a macroscopic deformation gradient $\mathbf{F}_0$ that is applied infinitely fast at $t = 0+$.

We are interested in solving (12)–(13) at $t = 0+$. To that end, we consider the ansatz

$$\begin{aligned} &\mathbf{y}(\mathbf{X}, t) = \mathbf{X} + \mathbf{u}_0(\mathbf{X}, t)\mathcal{H}(t), \\ &p(\mathbf{X}, t) = \mu_{\mathrm{m}} + \nu_{\mathrm{m}} + p_0(\mathbf{X}, t)\mathcal{H}(t), \\ &\mathbf{C}^v(\mathbf{X}, t) = \mathbf{I} + t\,\mathbf{C}_1^v(\mathbf{X}) + O(t^2) \end{aligned} \tag{32}$$

and introduce the notation

$$\mathbf{y}_0(\mathbf{X}) = \mathbf{y}(\mathbf{X}, 0+) = \mathbf{X} + \mathbf{u}_0(\mathbf{X}, 0+).$$

Recognizing from $(32)_3$ that

$$\dot{\mathbf{C}}^v = \mathbf{C}_1^v + O(t) \qquad \text{and} \qquad \mathbf{C}^{v\,-1} = \mathbf{I} - t\,\mathbf{C}_1^v + O(t^2),$$

it is a simple matter to solve equation (13) for the internal variable $\mathbf{C}^v(\mathbf{X}, t)$ to leading order to determine that

$$\mathbf{C}_1^v = \frac{\nu_{\mathrm{m}}}{\eta_{\mathrm{m}}}\left[\nabla\mathbf{y}_0^T\nabla\mathbf{y}_0 - \frac{1}{3}\left(\nabla\mathbf{y}_0 \cdot \nabla\mathbf{y}_0\right)\mathbf{I}\right].$$

It follows that at $t = 0+$ Eqs. (12) simplify to the boundary-value problem

$$\begin{cases} \mathrm{Div}\left[\left(1 - \theta_{\mathrm{i}}(\mathbf{X})\right)\left((\mu_{\mathrm{m}} + \nu_{\mathrm{m}})\nabla\mathbf{y}_0 - (\mu_{\mathrm{m}} + \nu_{\mathrm{m}} + p_0)\nabla\mathbf{y}_0^{-T}\right) + \theta_{\mathrm{i}}(\mathbf{X})\mu_{\mathrm{i}}\left(\nabla\mathbf{y}_0 - \nabla\mathbf{y}_0^{-T}\right)\right] = \mathbf{0}, & \mathbf{X} \in \Omega_0 \\ \det\nabla\mathbf{y}_0 = 1, & \mathbf{X} \in \Omega_0^{(\mathrm{m})} \\ \mathbf{y}_0(\mathbf{X}) = \mathbf{F}_0\mathbf{X}, & \mathbf{X} \in \partial\Omega_0 \end{cases} \tag{33}$$

for the deformation field $\mathbf{y}_0(\mathbf{X})$ and pressure field $p_0(\mathbf{X}, 0+)$.

After setting $\mu_{\mathrm{i}} = +\infty$, Eqs. (33) reduce to the governing equations for the homogenized elastic response of a random isotropic suspension of rigid inclusions, with characteristic function θ_{i}, embedded in a Gaussian rubber matrix with initial shear modulus $\mu_{\mathrm{m}} + \nu_{\mathrm{m}}$. In line with (29) hence, the macroscopic stress (10) corresponding to a macroscopic deformation gradient $\mathbf{F}_0$ that is applied infinitely fast at $t = 0+$ is approximately given by the relation

$$\mathbf{S}(t) = (\overline{\mu} + \overline{\nu})\,\mathbf{F}_0 - p\,\mathbf{F}_0^{-T} + O(t),$$

where, again, the effective material constants $\overline{\mu}$ and $\overline{\nu}$ are given by expressions $(23)_{1,2}$ and p stands for the arbitrary hydrostatic pressure associated with the incompressibility constraint $\det\mathbf{F}_0 = 1$.

5. The homogenized response at finite deformations in the absence of storage of elastic energy

Yet another basic limit for which Eqs. (12)–(13) are amenable to available methods of solution is when $\mu_{\mathrm{m}} = 0$ and $\nu_{\mathrm{m}} \to +\infty$, that is, when there is no storage of elastic energy and the rubber degenerates into a Newtonian fluid. In such a limit, the nonlinear viscoelasticity problem (12)–(13) reduces asymptotically — as one would expect from the rheological model in Fig. 1 — to the classical homogenization of the Stokes flow of an initially random isotropic *suspension of rigid inclusions in a Newtonian fluid*. The relevant calculations go as follows.

Set $\mu_{\mathrm{m}} = 0$ and consider solutions to (12)–(13) of the asymptotic form

$$\begin{aligned} &\mathbf{y}(\mathbf{X}, t) = \mathbf{y}_0(\mathbf{X}, t) + \nu_{\mathrm{m}}^{-1}\mathbf{y}_1(\mathbf{X}, t) + O(\nu_{\mathrm{m}}^{-2}), \\ &p(\mathbf{X}, t) = \nu_{\mathrm{m}} + p_0(\mathbf{X}, t) + O(\nu_{\mathrm{m}}^{-1}), \\ &\mathbf{C}^v(\mathbf{X}, t) = \mathbf{C}_0^v(\mathbf{X}, t) + \nu_{\mathrm{m}}^{-1}\mathbf{C}_1^v(\mathbf{X}, t) + O(\nu_{\mathrm{m}}^{-2}) \end{aligned} \tag{34}$$

in the limit as $\nu_{\mathrm{m}} \to +\infty$. Upon substitution of this ansatz in Eq. (13) for the internal variable $\mathbf{C}^v(\mathbf{X}, t)$, noting that

$$\dot{\mathbf{C}}^v = \dot{\mathbf{C}}_0^v + \nu_{\mathrm{m}}^{-1}\dot{\mathbf{C}}_1^v + O(\nu_{\mathrm{m}}^{-2}) \qquad \text{and} \qquad \mathbf{C}^{v\,-1} = \mathbf{C}_0^{v\,-1} - \nu_{\mathrm{m}}^{-1}\mathbf{C}_0^{v\,-1}\mathbf{C}_1^v\mathbf{C}_0^{v\,-1} + O(\nu_{\mathrm{m}}^{-2}),$$

it is a simple matter to solve the resulting asymptotic equations of $O(\nu_{\mathrm{m}})$ and $O(\nu_{\mathrm{m}}^0)$ to determine that

$$\mathbf{C}_0^v = \nabla\mathbf{y}_0^T\nabla\mathbf{y}_0 \tag{35}$$

and

$$\mathbf{C}_1^v = -\eta_{\mathrm{m}}\dot{\mathbf{C}}_0^v + \frac{1}{3}\left(\mathbf{C}_1^v\cdot\mathbf{C}_0^{v-1}\right)\mathbf{C}_0^v + \nabla\mathbf{y}_0^T\nabla\mathbf{y}_1 + \nabla\mathbf{y}_1^T\nabla\mathbf{y}_0 - \frac{1}{3}\left[\left(\nabla\mathbf{y}_0^T\nabla\mathbf{y}_1 + \nabla\mathbf{y}_1^T\nabla\mathbf{y}_0\right)\cdot\mathbf{C}_0^{v-1}\right]\mathbf{C}_0^v \tag{36}$$

for the first two terms in $(34)_3$. By making direct use now of (34), (35), and (36), together with a change of Lagrangian to Eulerian variables, the equation of $O(\nu_{\mathrm{m}}^0)$ emerging from (12) can be shown to reduce to the initial–boundary-value problem

$$\begin{cases} \operatorname{div}\left[\left(1-\chi_{\mathrm{i}}(\mathbf{x})\right)\left(\eta_{\mathrm{m}}(\nabla_{\mathbf{x}}\mathbf{v}+\nabla_{\mathbf{x}}\mathbf{v}^T)-q\mathbf{I}\right)+\chi_{\mathrm{i}}(\mathbf{x})\dfrac{\mu_{\mathrm{i}}}{\det\mathbf{F}_0}\left(\mathbf{F}_0\mathbf{F}_0^T-\mathbf{I}\right)\right]=\mathbf{0}, & (\mathbf{x},t)\in\Omega(t)\times[0,T] \\ \operatorname{tr}\nabla\mathbf{v}=0, & (\mathbf{x},t)\in\Omega^{(\mathrm{m})}(t)\times[0,T] \\ \mathbf{v}(\mathbf{x},t)=\dot{\mathbf{F}}(t)\mathbf{F}^{-1}(t)\mathbf{x}, & (\mathbf{x},t)\in\partial\Omega(t)\times[0,T] \end{cases} \tag{37}$$

coupled with the evolution equation

$$\begin{cases} \dfrac{\partial\mathbf{F}_0}{\partial t}+\mathbf{v}\cdot\nabla_{\mathbf{x}}\mathbf{F}_0=\nabla_{\mathbf{x}}\mathbf{v}\,\mathbf{F}_0, & (\mathbf{x},t)\in\Omega(t)\times[0,T] \\ \mathbf{F}_0(\mathbf{x},t)=\mathbf{F}(t), & (\mathbf{x},t)\in\partial\Omega(t)\times[0,T] \\ \mathbf{F}_0(\mathbf{x},0)=\mathbf{I}, & \mathbf{x}\in\Omega_0 \end{cases}$$

for the velocity field $\mathbf{v}\left(\mathbf{y}_0(\mathbf{X},t),t\right)=\dot{\mathbf{y}}_0(\mathbf{X},t)$, the deformation gradient $\mathbf{F}_0(\mathbf{y}_0(\mathbf{X},t),t)=\nabla\mathbf{y}_0(\mathbf{X},t)$, and the pressure field $q(\mathbf{x},t)$. In these last expressions, we have made use of the notation $\chi_{\mathrm{i}}(\mathbf{y}_0(\mathbf{X},t))=\theta_{\mathrm{i}}(\mathbf{X})$, $\nabla_{\mathbf{x}}\mathbf{F}_0(\mathbf{x},t)=\partial\mathbf{F}_0(\mathbf{x},t)/\partial\mathbf{x}$, and $\nabla_{\mathbf{x}}\mathbf{v}(\mathbf{x},t)=\partial\mathbf{v}(\mathbf{x},t)/\partial\mathbf{x}$.

When specialized to rigid inclusions, $\mu_{\mathrm{i}}=+\infty$, Eqs. (37) reduce to the governing equations for the homogenized *viscous* response of a suspension of rigid inclusions, with characteristic function χ_{i}, in a Newtonian fluid with viscosity η_{m} under conditions of Stokes flow and of no-slip between the inclusions and the fluid; see, e.g., Einstein (1906), Hashin (1963), Batchelor and Green (1972), Brady and Bossis (1988), Sierou and Brady (2001), and Stickel and Powell (2005). At any given *fixed* time $t\in[0,T]$, irrespectively of whether the spatial distribution of the inclusions remains random and isotropic along the applied deformation path, the problem (37) is thus mathematically equivalent to the *linear* elastostatics problem (18) that arises in the limit of small deformations. It then follows that the volume average

$$\mathbf{T}(t) := \frac{1}{|\Omega(t)|}\int_{\Omega(t)}\mathbf{T}(\mathbf{x},t)\mathrm{d}\mathbf{x}$$

of the pointwise Cauchy stress

$$\mathbf{T}(\mathbf{x},t)=\left(1-\chi_{\mathrm{i}}(\mathbf{x})\right)\left(\eta_{\mathrm{m}}(\nabla_{\mathbf{x}}\mathbf{v}+\nabla_{\mathbf{x}}\mathbf{v}^T)-q\mathbf{I}\right)+\chi_{\mathrm{i}}(\mathbf{x})\frac{\mu_{\mathrm{i}}}{\det\mathbf{F}_0}\left(\mathbf{F}_0\mathbf{F}_0^T-\mathbf{I}\right)$$

over the current configuration $\Omega(t)$ is simply given by the effective relation

$$\mathbf{T}(t)=\overline{\mathcal{M}}\,\mathbf{D}-p\mathbf{I}. \tag{38}$$

Here, p stands for the arbitrary hydrostatic pressure associated with the incompressibility constraint $\operatorname{tr}\nabla\mathbf{v}=0$, $\mathbf{D}(t)=\frac{1}{2}(\dot{\mathbf{F}}\mathbf{F}^{-1}+\mathbf{F}^{-T}\dot{\mathbf{F}}^T)$ denotes the macroscopic rate of deformation tensor, and the effective viscosity tensor $\overline{\mathcal{M}}$ is given by

$$\overline{\mathcal{M}}_{ijkl}=\frac{\eta_{\mathrm{m}}}{|\Omega(t)|}\int_{\Omega(t)}\left(1-\chi_{\mathrm{i}}(\mathbf{x})+k\chi_{\mathrm{i}}(\mathbf{x})\right)\mathcal{K}_{ijmn}\frac{\partial\gamma_{mkl}}{\partial x_n}(\mathbf{x})\mathrm{d}\mathbf{x}, \tag{39}$$

where, in line with (20) and (24), $k=+\infty$ and $\boldsymbol{\gamma}(\mathbf{x})$ is the concentration tensor that, together with $\boldsymbol{\sigma}(\mathbf{x})$, is solution of the linear "elastostatics" problem

$$\begin{cases} \dfrac{\partial}{\partial x_j}\left[\left(1-\chi_{\mathrm{i}}(\mathbf{x})+k\chi_{\mathrm{i}}(\mathbf{x})\right)\mathcal{K}_{ijmn}\dfrac{\partial\gamma_{mkl}}{\partial x_n}(\mathbf{x})+\delta_{ij}\sigma_{kl}(\mathbf{x})\right]=0, & \mathbf{x}\in\Omega(t) \\ \dfrac{\partial\gamma_{mkl}}{\partial x_m}(\mathbf{x})=0, & \mathbf{x}\in\Omega(t) \\ \gamma_{ikl}(\mathbf{x})=\delta_{ik}x_l, & \mathbf{x}\in\partial\Omega(t) \end{cases}$$

Recalling that for applied affine deformations $(12)_3$ with $\det\mathbf{F}(t)=1$ we have the connection $\mathbf{S}(t)=|\Omega_0|^{-1}\int_{\Omega_0}\mathbf{S}(\mathbf{X},t)\mathrm{d}\mathbf{X}=|\Omega(t)|^{-1}\int_{\Omega(t)}\mathbf{T}(\mathbf{x},t)\nabla_{\mathbf{x}}\mathbf{X}^T\,\mathrm{d}\mathbf{x}=\mathbf{T}(t)\mathbf{F}^{-T}(t)$, we can finally conclude from (38) that the macroscopic stress (10) in the limiting case when $\mu_{\mathrm{m}}=0$ and $\nu_{\mathrm{m}}\to+\infty$ is given by

$$\mathbf{S}(t)=\overline{\mathcal{M}}\left(\dot{\mathbf{F}}\mathbf{F}^{-1}\mathbf{F}^{-T}+\mathbf{F}^{-T}\dot{\mathbf{F}}^T\mathbf{F}^{-T}\right)-p\mathbf{F}^{-T}+O(\nu_{\mathrm{m}}^{-1}). \tag{40}$$

Remark 3. The response (40), or equivalently (38), is in general *non-Newtonian*. This is because the effective viscosity tensor (39) is not a constant but rather a function of the deformation history via the evolution in time of the characteristic function χ_{i} describing the microstructure. Indeed, the computation of the effective viscosity tensor (39) requires knowledge of the characteristic function χ_{i} in the current configuration. This amounts to keeping track of the evolution in space of all the inclusions in the suspension of

interest along the given loading path, which is a significant task. Regardless of how χ_{i} evolves in time, however, it is worth noting here for later use that the effective viscosity tensor (39) is bounded from below according to the Reuss bound (Willis, 1981)

$$\overline{\mathcal{M}} \geq 2\overline{\eta}_R \mathcal{K} \qquad \text{with} \qquad \overline{\eta}_R = \frac{\eta_{\mathrm{m}}}{1-c}, \tag{41}$$

where the inequality is meant in the sense of quadratic forms. For loading conditions for which the suspension remains isotropic, (39) is bounded from below according to the tighter Hashin–Shtrikman bound (Willis, 1981)

$$\overline{\mathcal{M}} \geq 2\overline{\eta}_{HS} \mathcal{K} \qquad \text{with} \qquad \overline{\eta}_{HS} = \frac{2+3c}{2(1-c)}\eta_{\mathrm{m}}. \tag{42}$$

6. The homogenized response at finite deformations for arbitrary loading conditions

As already noted above, for general macroscopic deformation gradients $\mathbf{F}(t)$, and general material constants μ_{m}, ν_{m}, η_{m}, the initial–boundary-value problem (12)–(13) defining the macroscopic response (10)–(11) of the suspension can only be solved numerically. In the sequel, we introduce a scheme to generate such numerical solutions. There are three challenges in doing so. The first one is to accurately describe the random isotropic microstructure of the suspension in a computationally accessible manner. The other two have to do with the selections of stable space and time discretizations capable of dealing with large deformations and the incompressibility of the rubber over the entire time domain $[0,T]$ of interest.

6.1. Weak form of the governing equations in a periodic setting

In practice, the characteristic function θ_{i} for a given suspension of interest is not expected to be fully available. But even if it were, as is well known, it would not be feasible from a computational point of view to deal with all the microstructural information that it would contain. A well-settled approach to circumvent this obstacle is that of idealizing the suspension as a periodic medium where the defining unit cell contains a random isotropic distribution of a sufficiently large but finite number N_{i} of inclusions that approximates the actual suspension; see, e.g., Gusev (1997), Michel et al. (1999), Segurado and Llorca (2002), Ghossein and Lévesque (2012), Lopez-Pamies et al. (2013b), and Shrimali et al. (2019). In such an approach, which we follow here, the pertinent calculations reduce to calculations over just the unit cell, Y_0 say. Precisely, the histories of the macroscopic first Piola Kirchhoff stress (10) and deformation gradient tensor (11) specialize to

$$\{\mathbf{S}(t),\ t\in[0,T]\}, \qquad \mathbf{S}(t) = \frac{1}{|Y_0|}\int_{Y_0} \mathbf{S}(\mathbf{X},t)\,\mathrm{d}\mathbf{X}$$

and

$$\{\mathbf{F}(t),\ t\in[0,T]\}, \qquad \mathbf{F}(t) = \frac{1}{|Y_0|}\int_{Y_0} \mathbf{F}(\mathbf{X},t)\,\mathrm{d}\mathbf{X},$$

while the initial–boundary-value problem (12)–(13), when rewritten in weak form, specializes to finding $\mathbf{y}(\mathbf{X},t)\in\mathcal{Y}$ and $p(\mathbf{X},t)\in\mathcal{P}$ such that

$$\begin{cases} \displaystyle\int_{Y_0}\left[\left(1-\theta_{\mathrm{i}}(\mathbf{X})\right)\left(\mu_{\mathrm{m}}\nabla\mathbf{y} - p\nabla\mathbf{y}^{-T} + \nu_{\mathrm{m}}\nabla\mathbf{y}\mathbf{C}^{v-1}\right) + \theta_{\mathrm{i}}(\mathbf{X})\mu_{\mathrm{i}}\left(\nabla\mathbf{y}-\nabla\mathbf{y}^{-T}\right)\right]\cdot\nabla\mathbf{w}\,\mathrm{d}\mathbf{X} = 0 \quad \forall\mathbf{w}\in\mathcal{Y}_0,\ t\in[0,T] \\ \displaystyle\int_{Y_0}\left[\left(1-\theta_{\mathrm{i}}(\mathbf{X})\right)(\det\nabla\mathbf{y}-1) + \theta_{\mathrm{i}}(\mathbf{X})\left(\det\nabla\mathbf{y} + \frac{\mu_{\mathrm{i}}}{p}\right)\right] q\,\mathrm{d}\mathbf{X} = 0 \quad \forall q\in\mathcal{P},\ t\in[0,T] \end{cases} \tag{43}$$

with $\mathbf{C}^v(\mathbf{X},t)$ defined by

$$\begin{cases} \dot{\mathbf{C}}^v(\mathbf{X},t) = \mathbf{G}\left(\nabla\mathbf{y}(\mathbf{X},t),\mathbf{C}^v(\mathbf{X},t)\right) \\ \qquad\qquad = \dfrac{\nu_{\mathrm{m}}}{\eta_{\mathrm{m}}}\left[\nabla\mathbf{y}^T\nabla\mathbf{y} - \frac{1}{3}\left(\nabla\mathbf{y}^T\nabla\mathbf{y}\cdot\mathbf{C}^{v-1}\right)\mathbf{C}^v\right], \quad (\mathbf{X},t)\in Y_0^{(\mathrm{m})}\times[0,T] \\ \mathbf{C}^v(\mathbf{X},0) = \mathbf{I}, \qquad\qquad \mathbf{X}\in Y_0^{(\mathrm{m})} \end{cases} . \tag{44}$$

In these expressions, $\mathcal{Y}$ and $\mathcal{P}$ stand for sufficiently large sets of admissible deformation $\mathbf{y}$ and pressure p fields that are consistent with the following periodicity conditions:

$$\mathbf{y}(\mathbf{X},t) = \mathbf{F}(t)\mathbf{X} + \check{\mathbf{y}}(\mathbf{X},t),\ \text{where } \check{\mathbf{y}} \text{ is } Y_0\text{−periodic}, \qquad \text{and} \qquad p \text{ is } Y_0\text{−periodic}. \tag{45}$$

Similarly, $\mathcal{Y}_0$ stands for a sufficiently large space of vector fields $\mathbf{w}$ that are Y_0-periodic. Moreover, $Y_0^{(\mathrm{m})}$ denotes the subdomain occupied by the rubber matrix in the unit cell Y_0 and, for later convenience, we have introduced the function $\mathbf{G}$ to denote the right-hand side of the evolution equation for $\mathbf{C}^v$.

6.2. Time discretization

Consider now a partition of the time interval under consideration $[0,T]$ into discrete times $t_k \in \{0 = t_0, t_1, \dots, t_m, t_{m+1}, \dots, t_M = T\}$. With help of the notation $\mathbf{y}_k(\mathbf{X}) = \mathbf{y}(\mathbf{X}, t_k)$, $\nabla\mathbf{y}_k(\mathbf{X}) = \nabla\mathbf{y}(\mathbf{X}, t_k)$, $p_k(\mathbf{X}) = p(\mathbf{X}, t_k)$, $\mathbf{C}^v_k(\mathbf{X}) = \mathbf{C}^v(\mathbf{X}, t_k)$, $\dot{\mathbf{C}}^v_k(\mathbf{X}) = \dot{\mathbf{C}}^v(\mathbf{X}, t_k)$, the governing Eqs. (43)–(44) at any given discrete time t_k take then the form

$$\begin{cases} \displaystyle\int_{Y_0} \left[\left(1 - \theta_{\mathtt{i}}(\mathbf{X})\right) \left(\mu_{\mathtt{m}} \nabla\mathbf{y}_k - p_k \nabla\mathbf{y}_k^{-T} + \nu_{\mathtt{m}} \nabla\mathbf{y}_k \mathbf{C}_k^{v\,-1} \right) + \theta_{\mathtt{i}}(\mathbf{X}) \mu_{\mathtt{i}} \left(\nabla\mathbf{y}_k - \nabla\mathbf{y}_k^{-T} \right) \right] \cdot \nabla\mathbf{w} \, \mathrm{d}\mathbf{X} = 0 \quad \forall \mathbf{w} \in \mathcal{Y}_0 \\ \displaystyle\int_{Y_0} \left[\left(1 - \theta_{\mathtt{i}}(\mathbf{X})\right) \left(\det \nabla\mathbf{y}_k - 1 \right) + \theta_{\mathtt{i}}(\mathbf{X}) \left(\det \nabla\mathbf{y}_k + \frac{\mu_{\mathtt{i}}}{p_k} \right) \right] q \, \mathrm{d}\mathbf{X} = 0 \quad \forall q \in \mathcal{P} \end{cases} \tag{46}$$

and

$$\dot{\mathbf{C}}^v_k(\mathbf{X}) = \mathbf{G}\left(\nabla\mathbf{y}_k(\mathbf{X}), \mathbf{C}^v_k(\mathbf{X}) \right), \tag{47}$$

where we emphasize that we are yet to choose an explicit or implicit time discretization for $\dot{\mathbf{C}}^v_k(\mathbf{X})$ in terms of $\mathbf{C}^v(\mathbf{X}, t)$.

6.3. Space discretization: conforming Crouzeix–Raviart finite elements

Having discretized the Eqs. (43)–(44) in time, the next step is to further discretize them in space. To this end, we begin by considering partitions ${}^hY_0 = \bigcup_{e=1}^{\mathtt{N}_e} \mathcal{E}^{(e)}$ of the unit cell Y_0 that comprise $\mathtt{N}_e$ non-overlapping quadratic simplicial elements $\mathcal{E}^{(e)}$. Given this partition, we look for approximate solutions ${}^h\mathbf{y}_k(\mathbf{X})$ and ${}^hp_k(\mathbf{X})$ of the deformation field $\mathbf{y}_k(\mathbf{X})$ and the pressure field $p_k(\mathbf{X})$ at time t_k in the finite dimensional subspace of quadratic Crouzeix–Raviart conforming finite elements; see, e.g., Chapter II in Girault and Raviart (1986), Chapter 8 in Boffi et al. (2012).

As elaborated in Section 5 and the Appendix in Lefèvre and Lopez-Pamies (2017b) in the more general setting of periodic homogenization of deformable dielectrics, it follows that ${}^h\mathbf{y}_k(\mathbf{X})$ and ${}^hp_k(\mathbf{X})$ admit the representations

$${}^h\mathbf{y}_k(\mathbf{X}) = \sum_{n=1}^{\mathtt{N}_n} {}^hN^{(n)}_{CR}(\mathbf{X}) \mathbf{y}^{(n)}_k \qquad \text{and} \qquad {}^hp_k(\mathbf{X}) = \sum_{l=0}^{4\mathtt{N}_e - 1} {}^hN^{(l)}_{P}(\mathbf{X}) p^{(l)}_k \tag{48}$$

in terms of the global degrees of freedom $\mathbf{y}^{(n)}_k$ and $p^{(l)}_k$ and associated global shape functions ${}^hN^{(n)}_{CR}(\mathbf{X})$ and ${}^hN^{(l)}_{P}(\mathbf{X})$ that result from the assembly process, where $\mathtt{N}_n$ stands for the total number of nodes in the partition ${}^hY_0$ of the unit cell Y_0. Physically, $\mathbf{y}^{(n)}_k$ corresponds to the deformation field ${}^h\mathbf{y}_k(\mathbf{X})$ at node (n) and time t_k, whereas $p^{(l)}_k$ corresponds to the value of the pressure ${}^hp_k(\mathbf{X})$ at the barycenters of the elements and the three components of its gradient at time t_k. By making use of the representations (48), analogous ones for the test functions $\mathbf{w}$ and q, and enforcing the periodicity conditions (45), Eqs. (46) reduce to a system of nonlinear algebraic equations for the degrees of freedom $\mathbf{y}^{(n)}_k$ and $p^{(l)}_k$ that depend on the values, say ${}^h\mathbf{C}^v_k$, of the internal variable $\mathbf{C}^v_k$ at the Gaussian quadrature points employed to carry out the integrals in (46). We write this system as

$$\mathcal{G}_1\left({}^h\mathbf{y}_k, {}^hp_k, {}^h\mathbf{C}^v_k; \mathbf{F}_k \right) = 0, \tag{49}$$

where we have included explicitly the parametric dependence on the applied macroscopic deformation gradient $\mathbf{F}_k = \mathbf{F}(t_k)$ at time t_k for clarity. Similarly, we write the coupled system of corresponding nonlinear algebraic equations that results from (47) for the internal variable $\mathbf{C}^v_k$ at the Gaussian quadrature points as

$$\mathcal{G}_2\left({}^h\mathbf{y}_k, {}^h\mathbf{C}^v_k, {}^h\dot{\mathbf{C}}^v_k; \mathbf{F}_k \right) = 0. \tag{50}$$

6.4. The solver: a Newton-like method staggered with a fifth-order explicit Runge–Kutta time integration

Having discretized the governing Eqs. (43)–(44) into the system of coupled nonlinear algebraic Eqs. (49)–(50) for the global degrees of freedom $\mathbf{y}^{(n)}_k$, $p^{(l)}_k$, and the internal variables ${}^h\mathbf{C}^v_k$ at the Gaussian quadrature points at time t_k, the final step is to solve these for given material constants $\mu_{\mathtt{m}}$, $\nu_{\mathtt{m}}$, $\eta_{\mathtt{m}}$, $\mu_{\mathtt{i}}$, given characteristic function $\theta_{\mathtt{i}}$, given applied macroscopic deformation gradient $\mathbf{F}(t)$, given time discretization $0 = t_0, t_1, \dots t_m, t_{m+1}, \dots, t_M = T$, and given space discretization ${}^hY_0$. We do so by following a staggered scheme, which involves solving the Eqs. (49) and (50) iteratively one after the other at every time step t_k until convergence is reached.

Precisely, the algorithm to solve (49) and (50) for $\mathbf{y}^{(n)}_k$, $p^{(l)}_k$, and ${}^h\mathbf{C}^v_k$ at t_k is as follows:

- *Step 0.* Set $r = 1$ and define appropriate tolerances $TOL_1, TOL_2 > 0$. For a given solution ${}^h\mathbf{y}_{k-1}$, ${}^hp_{k-1}$, and ${}^h\mathbf{C}^v_{k-1}$ at time t_{k-1}, define also ${}^h\mathbf{y}_{k,0} = {}^h\mathbf{y}_{k-1}$, ${}^hp_{k,0} = {}^hp_{k-1}$, and ${}^h\mathbf{C}^v_{k,0} = {}^h\mathbf{C}^v_{k-1}$.
- *Step 1.* Given the applied macroscopic deformation gradient $\mathbf{F}_k$, find ${}^h\mathbf{y}_{k,r}$ and ${}^hp_{k,r}$ such that

$$\mathcal{G}_1\left({}^h\mathbf{y}_{k,r}, {}^hp_{k,r}, {}^h\mathbf{C}^v_{k,r-1}; \mathbf{F}_k \right) = 0. \tag{51}$$

- *Step 2.* Having solved the sub-problem (51) for ${}^h\mathbf{y}_{k,r}$ and ${}^hp_{k,r}$, find ${}^h\mathbf{C}^v_{k,r}$ such that

$$\mathcal{G}_2\left({}^h\mathbf{y}_{k,r}, {}^hp_{k,r}, {}^h\mathbf{C}^v_{k,r}, {}^h\dot{\mathbf{C}}^v_{k,r}; \mathbf{F}_k\right) = 0. \tag{52}$$

- *Step 3.* If $\|\mathcal{G}_1({}^h\mathbf{y}_{k,r}, {}^hp_{k,r}, {}^h\mathbf{C}^v_{k,r}; \mathbf{F}_k)\|/\|\mathcal{G}_1({}^h\mathbf{y}_{k,0}, {}^hp_{k,0}, {}^h\mathbf{C}^v_{k,0}; \mathbf{F}_k)\| \leq TOL_1$ and $\|\mathcal{G}_2({}^h\mathbf{y}_{k,r}, {}^hp_{k,r}, {}^h\mathbf{C}^v_{k,r}, {}^h\dot{\mathbf{C}}^v_{k,r}; \mathbf{F}_k)\|/\|\mathcal{G}_2({}^h\mathbf{y}_{k,0}, {}^hp_{k,0}, {}^h\mathbf{C}^v_{k,0}, {}^h\dot{\mathbf{C}}^v_{k,0}; \mathbf{F}_k)\| \leq TOL_2$, then set ${}^h\mathbf{y}_k = {}^h\mathbf{y}_{k,r}$, ${}^hp_k = {}^hp_{k,r}$, ${}^h\mathbf{C}^v_k = {}^h\mathbf{C}^v_{k,r}$, and move to the next time step t_{k+1}; otherwise set $r \leftarrow r+1$ and go back to Step 1.

The sub-problem (51). In view of the fact that the internal variable ${}^h\mathbf{C}^v_{k,r-1}$ is kept fixed, the sub-problem (51) amounts to an incompressible finite elastostatics problem formulated with hybrid finite elements. Therefore, to solve for $\mathbf{y}^{(n)}_k$ and $p^{(l)}_k$, we make use of a Newton-like nonlinear method together with a direct solver (LU) for the resulting saddle-point linear system of equations at each Newton iteration. For problems of large size ($3\mathtt{N}_n + 4\mathtt{N}_e > 10^7$), instead of a direct solver, an iterative (Krylov subspace) solver with a suitable block preconditioner is required.

The sub-problem (52). The sub-problem (52) corresponds to a nonlinear system of first-order ODEs wherein the constraint of incompressibility $\det {}^h\mathbf{C}^v_{k,r} = 1$ is built-in. Because of the requirement of satisfying this nonlinear constraint along the entire time domain, as already noted in the Introduction, extreme care must be exercised in the choice of time-integration scheme (Simo, 1992). Based on a wide range of numerical experiments and comparisons with alternative implicit schemes, together with its proven success in integrating a variety of other types of nonlinear system of first-order ODEs (Lawson, 1967; Shu and Osher, 1988; Lefèvre et al., 2019), we make use of the explicit fifth-order Runge–Kutta scheme introduced by Lawson (1966). A key advantage of this scheme is that it allows to solve the sub-problem (52) explicitly. The solution reads

$${}^h\mathbf{C}^v_{k,r} = {}^h\mathbf{C}^v_{k-1} + \frac{\Delta t_k}{90}\left(7\mathbf{G}_1 + 32\mathbf{G}_3 + 12\mathbf{G}_4 + 32\mathbf{G}_5 + 7\mathbf{G}_6\right)$$

with

$$\begin{aligned}
\mathbf{G}_1 &= \mathbf{G}\left(\nabla^h\mathbf{y}_{k-1}, {}^h\mathbf{C}^v_{k-1}\right)\\
\mathbf{G}_2 &= \mathbf{G}\left(\frac{1}{2}\nabla^h\mathbf{y}_{k-1} + \frac{1}{2}\nabla^h\mathbf{y}_{k,r}, {}^h\mathbf{C}^v_{k-1} + \mathbf{G}_1\frac{\Delta t_k}{2}\right)\\
\mathbf{G}_3 &= \mathbf{G}\left(\frac{3}{4}\nabla^h\mathbf{y}_{k-1} + \frac{1}{4}\nabla^h\mathbf{y}_{k,r}, {}^h\mathbf{C}^v_{k-1} + (3\mathbf{G}_1 + \mathbf{G}_2)\frac{\Delta t_k}{16}\right)\\
\mathbf{G}_4 &= \mathbf{G}\left(\frac{1}{2}\nabla^h\mathbf{y}_{k-1} + \frac{1}{2}\nabla^h\mathbf{y}_{k,r}, {}^h\mathbf{C}^v_{k-1} + \mathbf{G}_3\frac{\Delta t_k}{2}\right)\\
\mathbf{G}_5 &= \mathbf{G}\left(\frac{1}{4}\nabla^h\mathbf{y}_{k-1} + \frac{3}{4}\nabla^h\mathbf{y}_{k,r}, {}^h\mathbf{C}^v_{k-1} + 3(-\mathbf{G}_2 + 2\mathbf{G}_3 + 3\mathbf{G}_4)\frac{\Delta t_k}{16}\right)\\
\mathbf{G}_6 &= \mathbf{G}\left(\nabla^h\mathbf{y}_{k,r}, {}^h\mathbf{C}^v_{k-1} + (\mathbf{G}_1 + 4\mathbf{G}_2 + 6\mathbf{G}_3 - 12\mathbf{G}_4 + 8\mathbf{G}_5)\frac{\Delta t_k}{7}\right),
\end{aligned}$$

where $\Delta t_k = t_k - t_{k-1}$ and where we recall that the function $\mathbf{G}$ is defined by $(44)_1$. A parametric study has indicated that time increments $\Delta t_k \leq 10^{-2}\tau_{\mathrm{m}}$ are sufficiently small to lead to converged solutions, at least for all the loading conditions that we have investigated in this work; recall that τ_{m} characterizes the relaxation time $(16)_2$ of the underlying rubber matrix. All the numerical results that are reported in the sequel have been generated with the time increment $\Delta t_k = 10^{-3}\tau_{\mathrm{m}}$.

7. Sample computational results for suspensions of monodisperse spherical inclusions

We now deploy the scheme proposed in the preceding section to generate solutions for the macroscopic response of a basic type of suspensions, that of monodisperse spherical inclusions.

For ease of implementation, we take the unit cell to be the unit cube $Y_0 = (0,1)^3$. For the construction of the random distributions of the inclusions in such unit cells, we make use of the algorithm introduced by Lubachevsky and Stillinger (1990). Although this algorithm allows to generate microstructures spanning the full range of volume fractions — from the dilute limit $c \searrow 0$ to the percolation threshold $c \nearrow c^* \approx 0.64$ (Scott, 1960; Lubachevsky et al., 1991) — we do not wish to deal with the computational demands of highly packed microstructures here and restrict our attention to the range $c \in [0, 0.25]$. A parametric study within such a range of volume fractions shows that microstructures with a total of $N_{\mathrm{i}} = 30$ inclusions per unit cell can render macroscopic behaviors that are essentially isotropic. Accordingly, all the results presented in the sequel correspond to computations based on unit cells containing $N_{\mathrm{i}} = 30$ inclusions. For the FE discretization of the constructed unit cells, we make use of the open-source mesh generator code NETGEN (Schöberl, 1997). Meshes with about 800,000 elements were checked to be sufficiently refined to deliver accurate solutions. Fig. 2 shows a representative unit cell at volume fraction $c = 0.15$ alongside its FE discretization with 729,849 elements.

Fig. 3 presents results for various types of uniaxial tension/compression loading conditions with $\mathbf{F}(t) = \mathsf{F}_{11}(t)(\mathbf{e}_1 \otimes \mathbf{e}_1 + \mathbf{e}_2 \otimes \mathbf{e}_2) + \mathsf{F}_{33}(t)\mathbf{e}_3 \otimes \mathbf{e}_3$ and $\mathbf{S}(t) = \mathsf{S}_{33}(t)\mathbf{e}_3 \otimes \mathbf{e}_3$, where $\{\mathbf{e}_i\}$ $i = 1,2,3$ stands for the laboratory frame of reference and $\mathsf{F}_{33}(t) > 0$ is prescribed. Specifically, Fig. 3(a) presents results for the stress $\mathsf{S}_{33}/\mu_{\mathrm{m}}$, normalized by the initial equilibrium shear modulus μ_{m} of the underlying rubber matrix, as a function of the stretch F_{33} for the case when F_{33} is first increased to $\mathsf{F}_{33} = 1.9$, subsequently

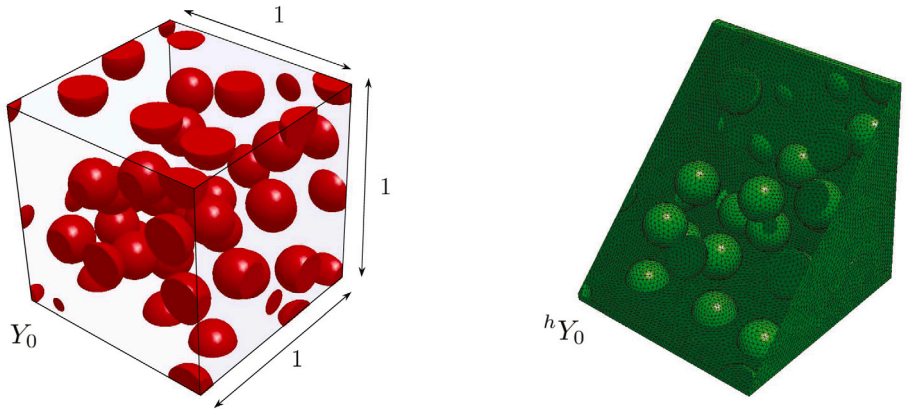

Fig. 2. Representative unit cell Y_0 containing $N_1 = 30$ randomly distributed spherical inclusions of the same size at volume fraction $c = 0.15$ and its FE discretization $^hY_0$ with 729,849 elements.

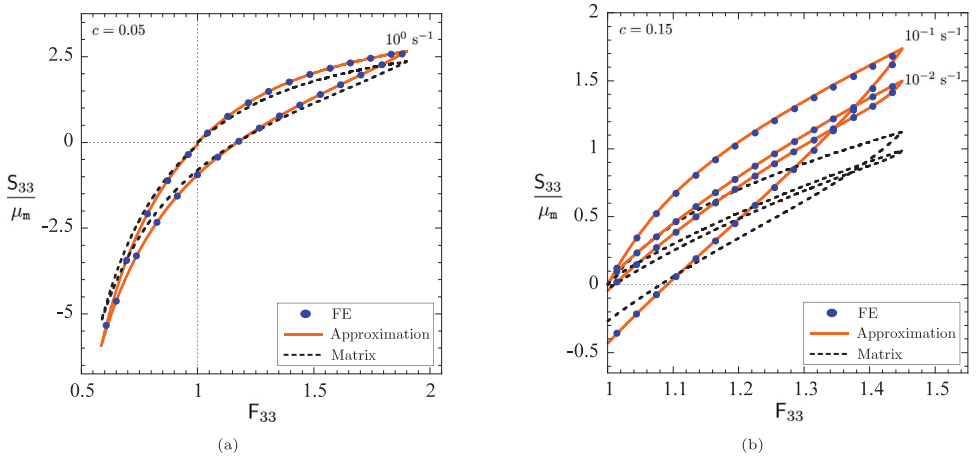

Fig. 3. Macroscopic response of suspensions of monodisperse spherical inclusions, at volume fractions $c = 0.05$ and 0.15, in a rubber matrix, with material constants $\nu_m = \mu_m$, $\tau_m = \eta_m/\nu_m = 1$ s, under various types of uniaxial tension/compression loading conditions. (a) Normalized stress–stretch relation for a uniaxial tension/compression loading/unloading cycle at constant stretch rate $|\dot{F}_{33}| = 10^0$ s^{-1}. (b) Normalized stress–stretch relation for a uniaxial tension loading/unloading cycle at constant stretch rates $|\dot{F}_{33}| = 10^{-2}$ and 10^{-1} s^{-1}.

decreased to $F_{33} = 1/1.9 = 0.53$, and then increased again to $F_{33} = 1$ at the constant stretch rate of $|\dot{F}_{33}| = 10^0$ s^{-1} for all three parts of the loading. Fig. 3(b) presents results for S_{33}/μ_m as a function of F_{33} for the case when F_{33} is increased to $F_{33} = 1.45$ and then decreased back to $F_{33} = 1$ at two different constant stretch rates, $|\dot{F}_{33}| = 10^{-2}$ and 10^{-1} s^{-1}. All the results in Fig. 3 pertain to suspensions wherein the rubber matrix has initial non-equilibrium shear modulus $\nu_m = \mu_m$, initial relaxation time[6] $\tau_m = 1$ s, and hence viscosity $\eta_m = \tau_m\nu_m = \mu_m$ s. Moreover, the results in Fig. 3(a) pertain to a suspension with $c = 0.05$ volume fraction of rigid inclusions, while those in Fig. 3(b) correspond to suspensions with $c = 0.15$.

Figs. 4(a) and (b) present results entirely analogous to those of Fig. 3 for loading conditions of simple shear with $\mathbf{F}(t) = F_{12}(t)\mathbf{e}_1 \otimes \mathbf{e}_2 + \mathbf{I}$, where $F_{12}(t)$ is prescribed. Moreover, Figs. 4(c) and (d) present results for a two-step relaxation test, wherein F_{12} is first increased to $F_{12} = 0.10$ at the constant shear rate of $|\dot{F}_{12}| = 10^{-1}$ s^{-1}, then held fixed for a time of $t = 10$ s, then increased to $F_{12} = 0.25$ at the same constant shear rate of $|\dot{F}_{12}| = 10^{-1}$ s^{-1}, and then held fixed again for the same amount of time $t = 10$ s. The results in Figs. 4(c) and (d) pertain to a suspension with $c = 0.25$ volume fraction of rigid inclusions.

Finally, Fig. 5 (Fig. 6) presents relaxation results entirely analogous to those of Figs. 4(c)–(d) for suspensions wherein the rubber matrix has initial non-equilibrium shear modulus $\nu_m = 0.1\mu_m$, $10\mu_m$ ($\nu_m = \mu_m$), initial relaxation time $\tau_m = 1$ s ($\tau_m = 0.1$, 10 s), and hence viscosity $\eta_m = \tau_m\nu_m = 0.1\mu_m$ s, $10\mu_m$ s ($\eta_m = \tau_m\nu_m = 0.1\mu_m$ s, $10\mu_m$ s).

[6] The choice of relaxation time $\tau_m = 1$ s implies actually that the time scale is normalized by the relaxation time τ_m of the rubber matrix, whatever this may be. Here and subsequently, for notational simplicity and without loss in generality, we use s as the unit of time.

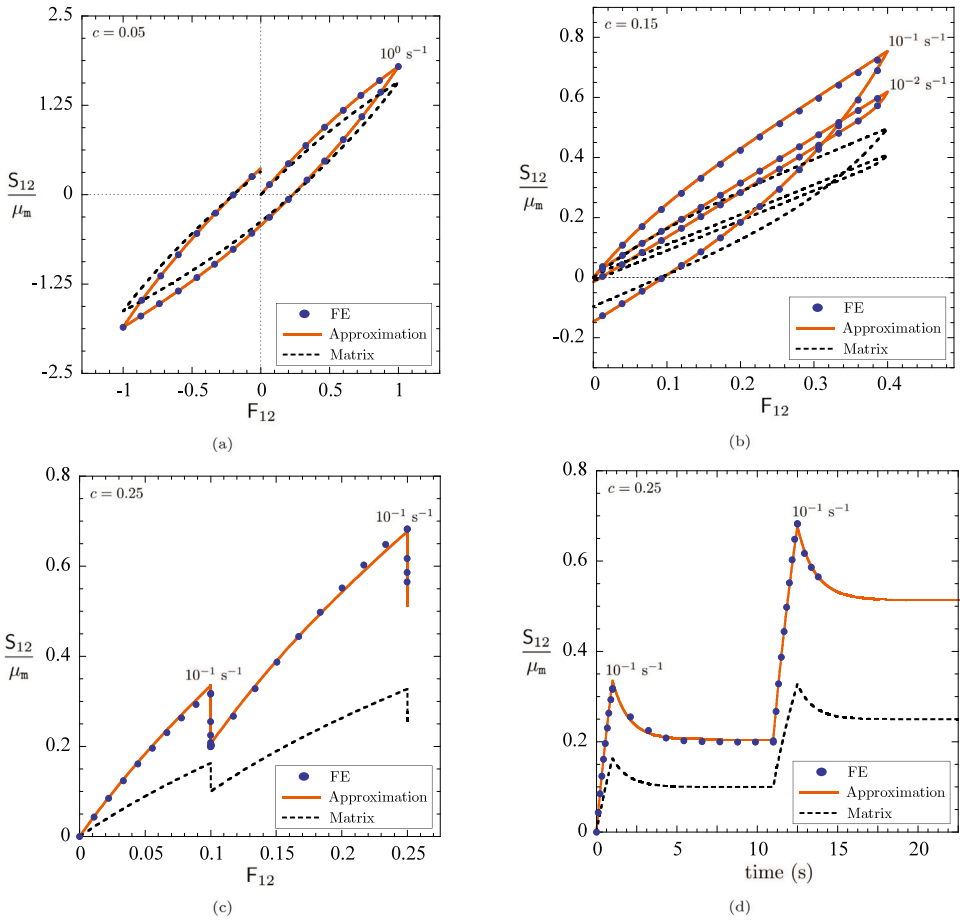

Fig. 4. Macroscopic response of suspensions of monodisperse spherical inclusions, at volume fractions $c = 0.05$, 0.15, 0.25, in a rubber matrix, with material constants $\nu_m = \mu_m$, $\tau_m = \eta_m/\nu_m = 1$ s, under various types of simple shear loading conditions. (a) Normalized stress–shear relation for a forward/backward loading/unloading shear cycle at constant rate $|\dot{F}_{12}| = 10^0$ s^{-1}. (b) Normalized stress–shear relation for a shear loading/unloading cycle at constant rates $|\dot{F}_{12}| = 10^{-2}$ and 10^{-1} s^{-1}. (c) Normalized stress–shear relation and (d) corresponding stress–time relation showing the two instances at which the shear is held fixed for a two-step relaxation test in simple shear where the shear is increased at the same constant rate $\dot{F}_{12} = 10^{-1}$ s^{-1} for the two loading steps.

For direct comparison with the computational FE results for the suspensions (solid circles), all the plots in Figs. 3 through 6 include the corresponding results for the unfilled rubber matrix (dashed lines). They also include the results based on the approximate solution (solid lines) introduced in the next section.

The above representative computational results provide a pivotal insight: the responses of the suspensions are qualitatively similar, albeit notably more nonlinear, to those of the underlying rubber matrix and thus suggest that they may feature the same type of short-range-memory behavior — as opposed to the generally expected long-range-memory behavior — for arbitrary finite deformations and loading conditions. The agreement shown by all the figures between the computational results and the approximate solution described next provide quantitative evidence that this may indeed be the case.

Before proceeding with the introduction of the approximate solution, it is important to emphasize two aspects about the above set of sample computational results. The first one is that they correspond to a range of loading conditions for which the nonlinear viscous dissipation of the underlying rubber matrix is fully probed (between the asymptotic limits of slow and fast rates discussed in Sections 4.1 and 4.2) given that the deformation rates considered are primarily of the same, of one more, and of one less order of magnitude than the relaxation time τ_m of the rubber. The second aspect that is important emphasizing is that the local deformations in the rubber are significantly larger than the applied macroscopic deformations because of the presence of the rigid inclusions, and so the results also fully probe the nonlinear (equilibrium and non-equilibrium) elasticity of the rubber.

8. An approximate solution

The asymptotic results presented in Section 3 have shown that the constitutive relation (10)–(11) that describes the macroscopic viscoelastic response of the suspensions of interest in this work is of identical functional form as that describing the underlying

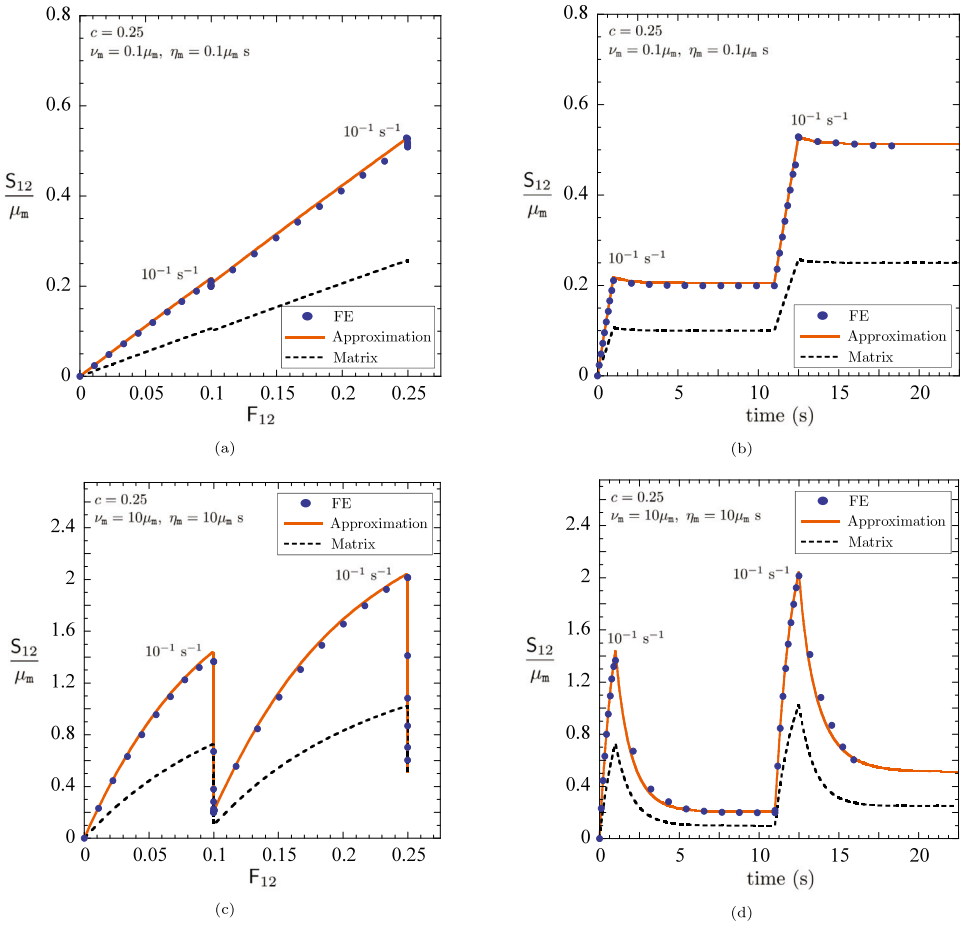

Fig. 5. Macroscopic response of suspensions of monodisperse spherical inclusions, at volume fraction $c = 0.25$, in a rubber matrix, with material constants $\nu_{\mathrm{m}} = 0.1\mu_{\mathrm{m}}$, $10\mu_{\mathrm{m}}$ and $\tau_{\mathrm{m}} = \eta_{\mathrm{m}}/\nu_{\mathrm{m}} = 1$ s, under a two-step relaxation test in simple shear where the shear is increased at the same constant rate $\dot{\mathsf{F}}_{12} = 10^{-1}$ s^{-1} for the two loading steps. (a)–(c) The normalized stress–shear relations. (b)–(d) The normalized stress-time relations.

rubber matrix in the limit of small deformations. Remarkably, the asymptotic results presented in Sections 4 and 5 together with the computational results presented in Section 7 suggest that *the same remains true at finite deformations, with the caveat that the viscosity of the suspensions is not a constant but rather a function of the deformation history*. Precisely, the results suggest that the macroscopic constitutive relation (10)–(11) can be cast within the two-potential framework as

$$\mathbf{S}(t) = \frac{\partial \Psi}{\partial \mathbf{F}}(\mathbf{F}, \mathbf{F}^v) - p\,\mathbf{F}^{-T} \tag{53}$$

with evolution equation

$$\begin{cases} \dfrac{\partial \Psi}{\partial \mathbf{F}^v}(\mathbf{F}, \mathbf{F}^v) + \dfrac{\partial \Phi}{\partial \dot{\mathbf{F}}^v}(\mathbf{F}, \mathbf{F}^v, \dot{\mathbf{F}}^v) = \mathbf{0} \\ \mathbf{F}^v(0) = \mathbf{I} \end{cases} \tag{54}$$

in terms of an effective free-energy function of the form

$$\Psi(\mathbf{F}, \mathbf{F}^v) = \begin{cases} \Psi^{\mathrm{Eq}}(\mathbf{F}) + \Psi^{\mathrm{NEq}}\left(\mathbf{F}\mathbf{F}^{v-1}\right) & \text{if} \quad \det \mathbf{F} = 1 \\ +\infty & \text{otherwise} \end{cases} \tag{55}$$

and an effective dissipation potential of the form

$$\Phi(\mathbf{F}, \mathbf{F}^v, \dot{\mathbf{F}}^v) = \begin{cases} \dfrac{1}{2}\dot{\mathbf{F}}^v\mathbf{F}^{v-1} \cdot \left[2\widetilde{\eta}(\mathbf{F}, \mathbf{F}^v)\,\boldsymbol{\mathcal{K}}\,\dot{\mathbf{F}}^v\mathbf{F}^{v-1}\right] & \text{if} \quad \mathrm{tr}\left(\dot{\mathbf{F}}^v\mathbf{F}^{v-1}\right) = 0 \\ +\infty & \text{otherwise} \end{cases}, \tag{56}$$

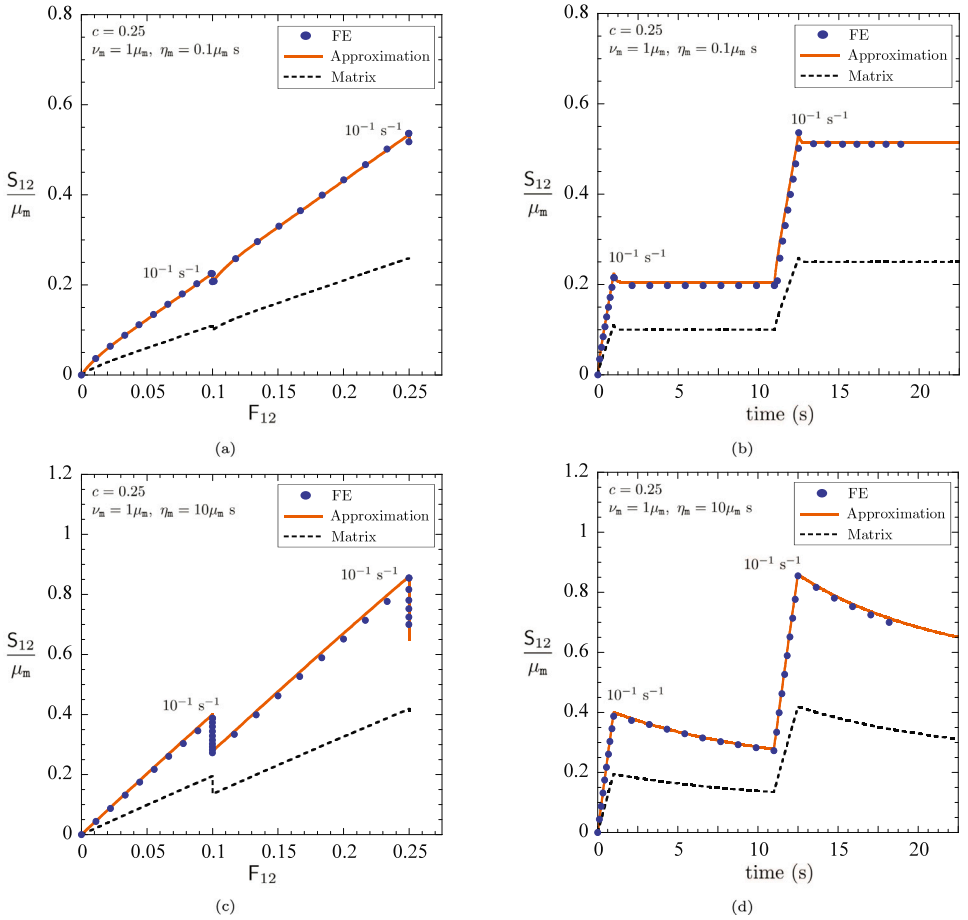

Fig. 6. Macroscopic response of suspensions of monodisperse spherical inclusions, at volume fraction $c = 0.25$, in a rubber matrix, with material constants $\nu_{\mathrm{m}} = \mu_{\mathrm{m}}$ and $\tau_{\mathrm{m}} = \eta_{\mathrm{m}}/\nu_{\mathrm{m}} = 0.1, 10$ s, under a two-step relaxation test in simple shear where the shear is increased at the same constant rate $\dot{\mathsf{F}}_{12} = 10^{-1}$ s^{-1} for the two loading steps. (a)–(c) The normalized stress–shear relations. (b)–(d) The normalized stress-time relations.

where $\mathbf{F}^{\upsilon}$ is the macroscopic internal variable of state that roughly corresponds to the "viscous part" of the macroscopic deformation gradient $\mathbf{F}$, Ψ^{Eq} and Ψ^{NEq} are the effective stored-energy functions that characterize, respectively, the elastic energy storage in the suspension at states of thermodynamic equilibrium and the additional elastic energy storage at non-equilibrium states, while the function $\widetilde{\eta}(\mathbf{F}, \mathbf{F}^{\upsilon})$ characterizes their effective viscosity.

Remark 4. At present, despite all the asymptotic and computational evidence pointing in that direction, we do not have a rigorous proof that the exact homogenized response of the suspension is indeed of the short-range-memory form described by Eqs. (53)–(56). The proof, if there is one, would appear to require establishing the direct link between the local fields $\mathbf{y}(\mathbf{X}, t)$ and $\mathbf{C}^{\upsilon}(\mathbf{X}, t)$ and the resulting internal macrovariable $\mathbf{F}^{\upsilon}$.

8.1. *Approximation of the effective free-energy functions* $\Psi^{\mathrm{Eq}}(\mathbf{F})$ *and* $\Psi^{\mathrm{NEq}}\left(\mathbf{F}\mathbf{F}^{\upsilon-1}\right)$

The results in Section 4 indicate in particular that Ψ^{Eq} and Ψ^{NEq} correspond to the free-energy functions that describe the homogenized *elastic* response of the given suspension of rigid inclusions, with characteristic function θ_{i}, embedded in Gaussian rubber matrices with initial shear moduli μ_{m} and ν_{m}, respectively. As already noted above around equation (29), simple yet accurate approximations for these effective free-energy functions are given by

$$\Psi^{\mathrm{Eq}}(\mathbf{F}) = \frac{\overline{\mu}}{2}\left[I_1 - 3\right] \qquad \text{and} \qquad \Psi^{\mathrm{NEq}}\left(\mathbf{F}\mathbf{F}^{\upsilon-1}\right) = \frac{\overline{\nu}}{2}\left[I_1^e - 3\right], \tag{57}$$

where

$$I_1 = \mathbf{F}\cdot\mathbf{F} = \operatorname{tr}\mathbf{C}, \qquad I_1^e = \mathbf{F}\mathbf{F}^{\upsilon-1}\cdot\mathbf{F}\mathbf{F}^{\upsilon-1} = \operatorname{tr}\left(\mathbf{C}\mathbf{C}^{\upsilon-1}\right)$$

with $\mathbf{C} = \mathbf{F}^T\mathbf{F}$ and $\mathbf{C}^{\upsilon} = \mathbf{F}^{\upsilon T}\mathbf{F}^{\upsilon}$, and where the effective material constants $\overline{\mu}$ and $\overline{\nu}$ are given by expressions $(23)_{1,2}$.

8.2. Approximation of the effective viscosity $\widetilde{\eta}(\mathbf{F}, \mathbf{F}^v)$

On the other hand, the asymptotic result in Section 5 indicates that the effective viscosity $\widetilde{\eta}$ is not necessarily a constant but rather a function of the evolution of the microstructure and hence of the deformation history. At time $t = 0$, as established in Section 3, when $\mathbf{F}(0) = \mathbf{F}^v(0) = \mathbf{I}$ and the microstructure of the given suspension is characterized by θ_{i}, we have that

$$\widetilde{\eta}(\mathbf{I}, \mathbf{I}) = \overline{\eta},$$

where $\overline{\eta}$ is the initial effective viscosity given by expression $(23)_3$. As the suspension is finitely deformed, the spatial distribution of the rigid inclusions evolves and, as a result, so possibly does its viscosity. A parametric analysis of a wide range of computational results, presented separately in the Appendix to avoid loss of continuity, has revealed that the formula

$$\widetilde{\eta}(\mathbf{F}, \mathbf{F}^v) = \breve{\eta}(I_1^v, J_2^v) = \widetilde{\eta}_\infty(I_1^v) + \frac{\widetilde{\eta}_0(I_1^v) - \widetilde{\eta}_\infty(I_1^v)}{1 + \left(K_1 J_2^v\right)^{\beta_1}} \tag{58}$$

with

$$\begin{cases} \widetilde{\eta}_0(I_1^v) = \overline{\eta} + K_2(I_1^{v\beta_2} - 3^{\beta_2})\overline{\eta} \\ \widetilde{\eta}_\infty(I_1^v) = \eta_{\mathrm{m}} + \tanh\left[K_3(I_1^{v\beta_3} - 3^{\beta_3})\right](\overline{\eta}_{HS} - \eta_{\mathrm{m}}) \end{cases}$$

and

$$I_1^v = \operatorname{tr} \mathbf{C}^v, \qquad J_2^v = \frac{\overline{\nu}^2}{2}\left[\mathbf{C}^{v-1}\mathbf{C}\cdot\mathbf{C}\mathbf{C}^{v-1} - \frac{1}{3}\left(\mathbf{C}\cdot\mathbf{C}^{v-1}\right)^2\right]$$

is able to describe fairly accurately the effective viscosity of all the suspensions that we have examined. Here, we recall that $\overline{\eta}$ and $\overline{\eta}_{HS}$ are given by expressions $(23)_3$ and $(42)_2$, while K_1, K_2, K_3, β_1, β_2, and β_3 are non-negative effective constants that depend on the materials constants μ_{m}, ν_{m}, η_{m} describing the viscoelastic behavior of the underlying rubber matrix and on the characteristic function θ_{i} describing the initial microstructure of the given suspension; while K_2, K_3, β_1, β_2, and β_3 are unitless, K_1 has units of $length^4/force^2$.

We close this subsection by emphasizing that the choice (58) is just one plausible approximation for the effective nonlinear viscosity of the suspensions. More refined approximations may be within reach by coupling the procedure outlined in the Appendix for the computational determination of the effective viscosity with emerging deep learning tools for ODEs, which appear to be particularly well suited for this endeavor.

8.3. The proposed approximate homogenization solution

Direct use of the approximations (57) and (58) in the effective free-energy function (55) and the effective dissipation potential (56), and of these in (53)–(54), leads to the following approximation of the macroscopic constitutive relation (10)–(11) for the suspension:

$$\mathbf{S}(t) = \overline{\mu}\,\mathbf{F} - p\,\mathbf{F}^{-T} + \overline{\nu}\,\mathbf{F}\mathbf{C}^{v-1}, \tag{59}$$

where p stands for the arbitrary hydrostatic pressure associated with the incompressibility constraint $\det \mathbf{F} = 1$ and the dependence on the macroscopic internal variable $\mathbf{F}^v$ enters through the symmetric combination $\mathbf{C}^v = \mathbf{F}^{vT}\mathbf{F}^v$ defined by the evolution equation

$$\begin{cases} \dot{\mathbf{C}}^v(t) = \dfrac{\overline{\nu}}{\breve{\eta}(I_1^v, J_2^v)}\left[\mathbf{C} - \dfrac{1}{3}\left(\mathbf{C}\cdot\mathbf{C}^{v-1}\right)\mathbf{C}^v\right] \\ \mathbf{C}^v(0) = \mathbf{I} \end{cases}. \tag{60}$$

The following remarks are in order.

Remark 5 (*The Effective Material Constants $\overline{\mu}$, $\overline{\nu}$, and Their Computation*)**.** The proposed approximate macroscopic response (59)–(60) contains two effective material constants, $\overline{\mu}$ and $\overline{\nu}$. Physically, they correspond to the initial shear moduli that describe the equilibrium and the non-equilibrium elasticity of the suspension at hand in the limit of small deformations. For convenience, we recall from Section 3 that they are given by the expressions

$$\overline{\mu} = g(c)\mu_{\mathrm{m}} \qquad \text{and} \qquad \overline{\nu} = g(c)\nu_{\mathrm{m}} \tag{61}$$

in terms of the corresponding initial shear moduli μ_{m} and ν_{m} of the underlying rubber matrix and of the enhancement function $g(c)$, which itself is given by expression (24) in terms of the characteristic function θ_{i} describing the initial microstructure of the suspension.

In principle, for a given characteristic function θ_{i} of interest, as already noted in Remark 1, the computation of the effective material constants (61) amounts to solving the linear elastostatics boundary-value problem (20) for the concentration tensor $\boldsymbol{\Gamma}(\mathbf{X})$ and to subsequently carrying out the volume average in (24) to determine the corresponding enhancement function $g(c)$. For practical purposes, as also already alluded to in Remark 1, it suffices to make use of the explicit formula (25) for $g(c)$ when dealing with suspensions with volume fractions in the range $c \in [0, 0.25]$.

Table 1
Values of the effective material constants K_1, K_2, K_3, β_1, β_2, and β_3 in the effective viscosity (58) for the suspensions of monodisperse spherical inclusions examined in Section 7.

ν_m/μ_m	τ_m(s)	c	K_1/μ_m	K_2	K_3	β_1	β_2	β_3
1	1	0.05	2.301	0.061	0.934	2.109	2.322	0.823
1	1	0.15	2.740	0.520	0.909	0.975	1.619	0.540
1	1	0.25	1.471	0.520	0.910	1.189	2.011	0.550
0.1	1	0.05	2.023	0.873	0.923	2.109	2.322	0.823
10	1	0.05	0.031	0.076	0.932	2.109	2.322	0.823
0.1	1	0.15	2.740	0.518	0.909	0.975	1.619	0.540
10	1	0.15	2.637	0.782	1.128	0.975	1.619	0.540
0.1	1	0.25	1.028	0.257	1.000	1.189	2.011	0.550
10	1	0.25	0.295	1.062	1.064	1.189	2.011	0.550
1	0.1	0.05	2.022	0.001	0.923	2.109	2.322	0.823
1	10	0.05	0.680	0.000	0.924	2.109	2.322	0.823
1	0.1	0.15	2.734	0.019	0.909	0.975	1.619	0.540
1	10	0.15	2.716	0.031	0.915	0.975	1.619	0.540
1	0.1	0.25	1.647	0.000	0.987	1.189	2.011	0.550
1	10	0.25	1.334	0.922	0.997	1.189	2.011	0.550

Remark 6 (*The Effective Material Function $\check{\eta}(I_1^v, J_2^v)$ and its Computation*)**.** In addition to the two effective material constants $\overline{\mu}$ and $\overline{\nu}$, the proposed approximate macroscopic response (59)–(60) contains one effective material function, $\check{\eta}(I_1^v, J_2^v)$. Physically, again, this function characterizes the nonlinear viscosity of the suspension.

Specifically, the proposed effective viscosity (58) is a function of two invariants, I_1^v and J_2^v. As elaborated in the Appendix, the latter provides a measure of the "viscous part" of the macroscopic stress $\mathbf{S}$ in the suspension, while the former provides a measure of the "viscous part" of the macroscopic deformation gradient $\mathbf{F}$. According to (58), the larger the value of J_2^v, the smaller the value of the effective viscosity. This is commonly referred to as shear thinning, a behavior that falls squarely within that of numerous suspensions of rigid inclusions in Newtonian fluids, which, again, in the present more general setting of finite viscoelasticity corresponds to the limit when $\mu_m = 0$ and $\nu_m \to +\infty$; see, e.g., Krieger and Dougherty (1959), Cross (1970), Krieger (1972), Jeffrey and Acrivos (1976), and Stickel and Powell (2005). The shear thinning described by (58) is deformation dependent via I_1^v.

Concerning its computation, the effective viscosity (58) contains nine effective material constants, $\overline{\eta} = g(c)\eta_m$, $\overline{\eta}_{HS} = (2 + 3c)\eta_m/2(1-c)$, $\overline{\nu} = g(c)\nu_m$, K_1, K_2, K_3, β_1, β_2, and β_3. The computation of $\overline{\eta}$ requires knowledge of the same enhancement coefficient $g(c)$ associated with the effective elastic constant $\overline{\nu}$ discussed in the preceding remark, whereas that of $\overline{\eta}_{HS}$ only requires knowledge of the volume fraction c of inclusions in the suspension. The computation of the $K's$ and $\beta's$, which needs to be carried out numerically, is presented in Appendix. Table 1 logs the values of the $K's$ and $\beta's$ for the suspensions of monodisperse spherical inclusions studied in Section 7.

Remark 7 (*The Limit of Small Deformations*)**.** In the limit of small deformations as $\|\mathbf{F}(t) - \mathbf{I}\| = \|\mathbf{H}(t)\| \to 0$, a calculation akin to that detailed in Section 3 shows that the macroscopic response (59)–(60) reduces asymptotically to the exact solution (21)–(22).

Remark 8 (*Finite Deformations Applied Infinitesimally Slowly and "Infinitely" Fast*)**.** In the limit of finite deformations that are applied either infinitesimally slowly or "infinitely" fast, the macroscopic response (59)–(60) reduces to

$$\mathbf{S}(t) = \overline{\mu}\,\mathbf{F} - p\,\mathbf{F}^{-T}$$

and

$$\mathbf{S}(t) = (\overline{\mu} + \overline{\nu})\,\mathbf{F} - p\,\mathbf{F}^{-T},$$

respectively. As already noted in Section 4, these results are not exact in general, but they are very accurate for arbitrary deformations.

Remark 9 (*The Absence of Storage of Elastic Energy*)**.** In the limit as $\mu_m = 0$ and $\nu_m \to +\infty$, when the underlying rubber matrix degenerates into a Newtonian fluid, taking $K_2 \searrow 0$ and $K_3 \to +\infty$, a calculation akin to that presented in Section 5 shows that the macroscopic response (59)–(60), when written in terms of the macroscopic Cauchy stress $\mathbf{T} = \mathbf{S}\mathbf{F}^T$, specializes to

$$\mathbf{T}(t) = \left(\overline{\eta}_{HS} + \frac{\overline{\eta} - \overline{\eta}_{HS}}{1 + (K_1 J_2)^{\beta_1}}\right)\mathbf{D} - p\mathbf{I}, \tag{62}$$

where, again, $\mathbf{D} = \frac{1}{2}(\dot{\mathbf{F}}\mathbf{F}^{-1} + \mathbf{F}^{-T}\dot{\mathbf{F}}^T)$ stands for the macroscopic rate of deformation tensor and

$$J_2 = \frac{1}{2}\mathrm{tr}\mathbf{T}_D^2$$

denotes the second principal invariant of the deviatoric Cauchy stress $\mathbf{T}_D = \mathbf{T} - \frac{1}{3}(\mathrm{tr}\mathbf{T})\mathbf{I}$. The constitutive response (62) is that of a non-Newtonian fluid with shear thinning of the classical form introduced by Krieger and Dougherty (1959). While the result (62) is

not an exact solution in general, it has been established to provide a fairly accurate approximation, at least for simple shear flows; see Krieger (1972) and Stickel and Powell (2005), for example.

Remark 10 (*Accuracy*)**.** By construction, as noted in the preceding three remarks, the proposed approximate macroscopic response (59)–(60) is exact in the limit of small deformations and, albeit not exact, very accurate for finite deformations that are applied either slowly or fast, as well as for the case when the underlying rubber matrix approaches the behavior of a Newtonian fluid. Comparisons with a wide spectrum of computational results, a representative sample of which have been presented in Section 7 above, suggest that (59)–(60) remains accurate for arbitrary finite deformations, loading conditions, material constants μ_{m}, ν_{m}, η_{m} describing the viscoelastic behavior of the underlying rubber matrix, and microstructures, as described by the characteristic function θ_{i}.

Remark 11 (*Numerical Implementation*)**.** From a further practical point of view, we close this section by remarking that the same numerical scheme presented in Section 6 applies *mutatis mutandis* to the constitutive relation (59)–(60) in order to solve macroscopic initial–boundary-value problems of interest.

9. Final comments

The homogenization results worked out in this paper for the viscoelastic response of suspensions of rigid inclusions in rubber under finite quasistatic deformations are striking — at least at first sight — on two counts. First, contrary to the generally expected long-range-memory behavior, the response appears to exhibit a short-range-memory behavior akin to that of the underlying rubber matrix. What is more, the effective viscosity of the suspensions exhibits shear thinning, this in spite of the fact that the viscosity of the underlying rubber is constant.

Much like for suspensions of rigid inclusions in Newtonian fluids, the shear-thinning viscosity can be attributed to the evolution of microstructure that invariably occurs under finite deformations. On the other hand, the apparent short-range-memory behavior is likely the manifestation of the fact that there is only one relaxation mechanism in the suspensions: the shear relaxation of the rubber.

A single mechanism of relaxation. To illustrate the concept of a single mechanism of relaxation in more precise terms and to gain insight into its implications, consider an isotropic *linear* viscoelastic composite material characterized by the pointwise constitutive relation

$$\mathbf{S}(\mathbf{X},t)=\int_{-\infty}^{t}\mathbf{L}(\mathbf{X},t-\tau)\frac{\partial\mathbf{H}}{\partial\tau}(\mathbf{X},\tau)\mathrm{d}\tau\qquad\text{with}\qquad\mathbf{L}(\mathbf{X},t)=2\mu(\mathbf{X})f(t)\boldsymbol{\mathcal{K}}+3\kappa(\mathbf{X})f(t)\boldsymbol{\mathcal{J}},\tag{63}$$

where, using the same notation employed in Section 3 above, $\mathbf{L}(\mathbf{X},t)$ stands for the relaxation function of the material and $\boldsymbol{\mathcal{J}}=\boldsymbol{\mathcal{I}}-\boldsymbol{\mathcal{K}}$ is the standard volumetric orthogonal projection tensor. While arbitrarily heterogeneous through $\mu(\mathbf{X})$ and $\kappa(\mathbf{X})$, the constitutive relation (63) has a single mechanism of relaxation characterized by the function $f(t)$. Its Laplace transform reads

$$\widehat{\mathbf{S}}(\mathbf{X},s)=s\widehat{f}(s)\left[2\mu(\mathbf{X})\boldsymbol{\mathcal{K}}+3\kappa(\mathbf{X})\boldsymbol{\mathcal{J}}\right]\widehat{\mathbf{H}}(\mathbf{X},s).\tag{64}$$

It follows that the s-dependent term $s\widehat{f}(s)$ in (64) can be factored out of the governing equation $\mathrm{Div}\,\widehat{\mathbf{S}}(\mathbf{X},s)=\mathbf{0}$ and hence that the resulting homogenized response (see Section 3) exhibits the same time-dependent behavior as its local response, precisely,

$$\mathbf{S}(t)=\int_{-\infty}^{t}\mathbf{L}(t-\tau)\frac{\partial\mathbf{H}}{\partial\tau}(\tau)\mathrm{d}\tau\qquad\text{with}\qquad\mathbf{L}(t)=2\widetilde{\mu}f(t)\boldsymbol{\mathcal{K}}+3\widetilde{\kappa}f(t)\boldsymbol{\mathcal{J}}.\tag{65}$$

The result (65) makes it plain that the two-phase suspensions of rigid inclusions in isotropic incompressible rubber that we have investigated in this paper are but one example of composite materials with a single mechanism of relaxation; one where $\kappa(\mathbf{X})=+\infty$. The result (65) also makes it plain that any such material would exhibit a short-range-memory homogenized response if its local behavior is of short-range memory.

Beyond the limit of small deformations just outlined, based on the asymptotic and computational results presented in this paper, and on additional computational results not included here for conciseness, we conjecture that viscoelastic composite materials featuring a single mechanism of relaxation, after homogenization, will continue to exhibit a single mechanism of relaxation even when finitely deformed.

Non-Gaussian rubber with nonlinear viscosity. As alluded to in the Introduction, the idealizations of Gaussian elasticity and constant viscosity do not apply to actual rubber, or, more generally, to elastomers at large, at sufficiently large deformations and deformation rates. Indeed, actual elastomers feature non-Gaussian elasticity and nonlinear viscosity, the latter being typically of shear-thinning type; see Gent (1962), Khan and Lopez-Pamies (2002), Amin et al. (2006), Kumar and Lopez-Pamies (2016), and Chockalingam et al. (2021) for example.

Preliminary results entirely analogous to the ones presented here but for suspensions of rigid inclusions in a certain type of non-Gaussian rubber with nonlinear viscosity have indicated that their homogenized response still remains described by a model of the form (53)–(56), with the caveat that the effective free energies in (55) are non-Gaussian and the effective nonlinear viscosity in the dissipation potential (56) contains contributions from the nonlinear viscosity of the underlying rubber *and* from the evolution of the microstructure. This behavior falls squarely within the conjecture made above for materials with a single mechanism of relaxation. Plans to continue the study of the homogenized response of these more general systems and its comparison with experiments are underway and will be reported elsewhere.

CRediT authorship contribution statement

Kamalendu Ghosh: Conceptualization, Methodology, Software, Writing - review & editing. **Bhavesh Shrimali:** Methodology, Software, Writing - review & editing. **Aditya Kumar:** Methodology, Software, Writing - review & editing. **Oscar Lopez-Pamies:** Conceptualization, Methodology, Supervision, Writing - original draft, Writing - review & editing, Funding acquisition.

Declaration of competing interest

The authors declare that they have no known competing financial interests or personal relationships that could have appeared to influence the work reported in this paper.

Acknowledgment

Support for this work by the National Science Foundation, USA through the Grant DMREF–1922371 is gratefully acknowledged.

Appendix. The functional form (58) of the effective viscosity

With some abuse of notation, assuming that the homogenized response (53) of the suspension depends on the macroscopic internal variable $\mathbf{F}^v$ only through its symmetric combination $\mathbf{C}^v = \mathbf{F}^{vT}\mathbf{F}^v$ as does its local counterpart (8), we begin by rewriting the material function $\widetilde{\eta}(\mathbf{F}, \mathbf{F}^v)$ in (56) describing the effective viscosity of the suspension as

$$\widetilde{\eta}(\mathbf{F}, \mathbf{F}^v) = \widetilde{\eta}(\mathbf{F}, \mathbf{C}^v).$$

Now, from material frame indifference and material symmetry requirements, we have that

$$\widetilde{\eta}(\mathbf{QFK}, \mathbf{K}^T\mathbf{C}^v\mathbf{K}) = \widetilde{\eta}(\mathbf{F}, \mathbf{C}^v) \qquad \forall\, \mathbf{Q}, \mathbf{K} \in Orth^+. \tag{66}$$

With some further abuse of notation, it follows from the constraint (66) that the function $\widetilde{\eta}(\mathbf{F}, \mathbf{C}^v)$ admits the representation

$$\widetilde{\eta}(\mathbf{F}, \mathbf{C}^v) = \widetilde{\eta}(\mathbf{C}, \mathbf{C}^v) = \widetilde{\eta}(I_1, I_2, I_1^v, I_2^v, I_4^v, I_5^v, I_6^v, I_7^v) \tag{67}$$

in terms of the eight standard invariants

$$\begin{aligned} &I_1 = \mathrm{tr}\,\mathbf{C}, && I_2 = \mathrm{tr}\,\mathbf{C}^2, && I_1^v = \mathrm{tr}\,\mathbf{C}^v, && I_2^v = \mathrm{tr}\,\mathbf{C}^{v2}, \\ &I_4^v = \mathrm{tr}\,(\mathbf{C}\mathbf{C}^v), && I_5^v = \mathrm{tr}\left(\mathbf{C}^2\mathbf{C}^v\right), && I_6^v = \mathrm{tr}\left(\mathbf{C}\mathbf{C}^{v2}\right), && I_7^v = \mathrm{tr}\left(\mathbf{C}^2\mathbf{C}^{v2}\right) \end{aligned} \tag{68}$$

of the macroscopic right Cauchy–Green deformation tensor $\mathbf{C}$ and $\mathbf{C}^v$; see, e.g., Boehler (1987).

At this stage, the crux of the matter is to determine the precise form of (67) in terms of the eight invariants (68). In principle, this could be accomplished by generating computational results for the macroscopic response of the suspension of interest under loading conditions that vary one of the eight invariants (68) at a time while keeping the other seven fixed and then having the proposed approximate macroscopic response (53) match those results thereby determining the corresponding effective viscosity (67). While conceptually simple, the computational cost of this approach is prohibitive. Here, we follow a more pragmatic approach that hinges on the physically-based premise that the effective viscosity of any given suspension depends primarily on two quantities: (*i*) the "viscous part" of the macroscopic deformation gradient $\mathbf{F}$ and (*ii*) the "viscous part" of the macroscopic stress $\mathbf{S}$. The simplest invariant in (68) that provides a measure of the viscous part of the macroscopic deformation gradient $\mathbf{F}$ is I_1^v. To identify a corresponding invariant that provides a measure of the viscous part of the macroscopic stress $\mathbf{S}$, we first define

$$\mathbf{T}_D^v = 2\widetilde{\eta}(\mathbf{C}, \mathbf{C}^v)\mathbf{D}^v = \widetilde{\eta}(\mathbf{C}, \mathbf{C}^v)\left(\dot{\mathbf{F}}^v\mathbf{F}^{v-1} + \mathbf{F}^{v-T}\dot{\mathbf{F}}^{vT}\right) = \overline{v}\left[\mathbf{F}^{v-T}\mathbf{C}\mathbf{F}^{v-1} - \frac{1}{3}\left(\mathbf{C}\cdot\mathbf{C}^{v-1}\right)\mathbf{I}\right] \tag{69}$$

as the viscous part of the Cauchy stress $\mathbf{T} = \mathbf{S}\mathbf{F}^T$ in the suspension; note that relation (69) is the evolution equation (60) multiplied by $\mathbf{F}^{v-T}$ from the left, $\mathbf{F}^{v-1}$ from the right, and rewritten for an arbitrary effective viscosity $\widetilde{\eta}(\mathbf{C}, \mathbf{C}^v)$. The second principal invariant of the stress (69) is given by

$$J_2^v = \frac{1}{2}\mathrm{tr}\,\mathbf{T}_D^{v\,2} = \frac{\overline{v}^2}{2}\left[\mathbf{C}^{v-1}\mathbf{C}\cdot\mathbf{C}\mathbf{C}^{v-1} - \frac{1}{3}\left(\mathbf{C}\cdot\mathbf{C}^{v-1}\right)^2\right]$$

and provides the stress measure that we are after. When rewritten in terms of the invariants (68), it takes the form

$$J_2^v = \frac{\overline{v}^2}{2}\left[I_1^v\left(I_2 - I_1^2\right) + 2I_1I_4^v - 2I_5^v + \frac{1}{6}\left(I_1\left(I_1^{v2} - I_2^v\right) - 2I_1^vI_4^v + 2I_6^v\right)^2\right]. \tag{70}$$

We henceforth take I_1^v and the combination (70) as the variables that quantify the viscous part of the macroscopic deformation gradient $\mathbf{F}$ and the viscous part of the macroscopic stress $\mathbf{S}$ in the suspension and thus write

$$\widetilde{\eta}(I_1, I_2, I_1^v, I_2^v, I_4^v, I_5^v, I_6^v, I_7^v) = \breve{\eta}(I_1^v, J_2^v). \tag{71}$$

In view of the connection (70), note that the proposed prescription (71) depends on all invariants (68) save for I_7^v.

Having settled on the functional dependence (71) for the effective viscosity, the next step is to determine its precise form. We do so by generating computational results — via the FE scheme presented in Section 6 — for the macroscopic response of the suspension of interest under loading conditions that vary J_2^v and I_1^v independently and then having the proposed approximate macroscopic response (59) with (60) match those results thereby determining the value of the effective viscosity $\breve{\eta}(I_1^v, J_2^v)$ as a function of its arguments.

Precisely, we consider loading conditions of the form

$$\mathbf{F}(t) = \mathbf{F}_0 + \mathcal{H}(t)\left(\mathbf{F}_1 - \mathbf{F}_0\right), \tag{72}$$

where $\mathcal{H}(t)$ stands for the Heaviside function (31); this is a generalization of the loading (30) considered in Section 4.2 in that a macroscopic deformation gradient $\mathbf{F}_1$ is applied infinitely fast starting from a state in equilibrium that is not necessarily undeformed but rather described by the macroscopic deformation gradient $\mathbf{F}_0$. Under such loading conditions, the approximate macroscopic response (59)–(60) can be written explicitly in the asymptotic limit as $t \to 0+$. The result reads

$$\mathbf{S}(t) = \overline{\mu}\,\mathbf{F}_1 - p\,\mathbf{F}_1^{-T} + \overline{\nu}\,\mathbf{F}_1\mathbf{C}_0^{-1} - t\,\frac{\overline{\nu}^2}{\breve{\eta}\left(I_1^v|_{0+}, J_2^v|_{0+}\right)}\left(1 - \frac{1}{3}\mathbf{C}_1\cdot\mathbf{C}_0^{-1}\right)\mathbf{F}_1\mathbf{C}_0^{-1}\mathbf{C}_1\mathbf{C}_0^{-1} + O(t^2), \tag{73}$$

where $\mathbf{C}_0 = \mathbf{F}_0^T\mathbf{F}_0$, $\mathbf{C}_1 = \mathbf{F}_1^T\mathbf{F}_1$, and the arguments in the viscosity function are given by

$$I_1^v|_{0+} = \operatorname{tr}\mathbf{C}_0 \qquad \text{and} \qquad J_2^v|_{0+} = \frac{\overline{\nu}^2}{2}\left[\mathbf{C}_0^{-1}\mathbf{C}_1\cdot\mathbf{C}_1\mathbf{C}_0^{-1} - \frac{1}{3}\left(\mathbf{C}_1\cdot\mathbf{C}_0^{-1}\right)^2\right].$$

It follows from (73) that

$$\breve{\eta}\left(I_1^v|_{0+}, J_2^v|_{0+}\right) = -\frac{\overline{\nu}^2}{\operatorname{tr}\dot{\mathbf{S}}(0+)}\left(1 - \frac{1}{3}\mathbf{C}_1\cdot\mathbf{C}_0^{-1}\right)\mathbf{F}_1^T\mathbf{C}_0^{-1}\cdot\mathbf{C}_0^{-1}\mathbf{C}_1. \tag{74}$$

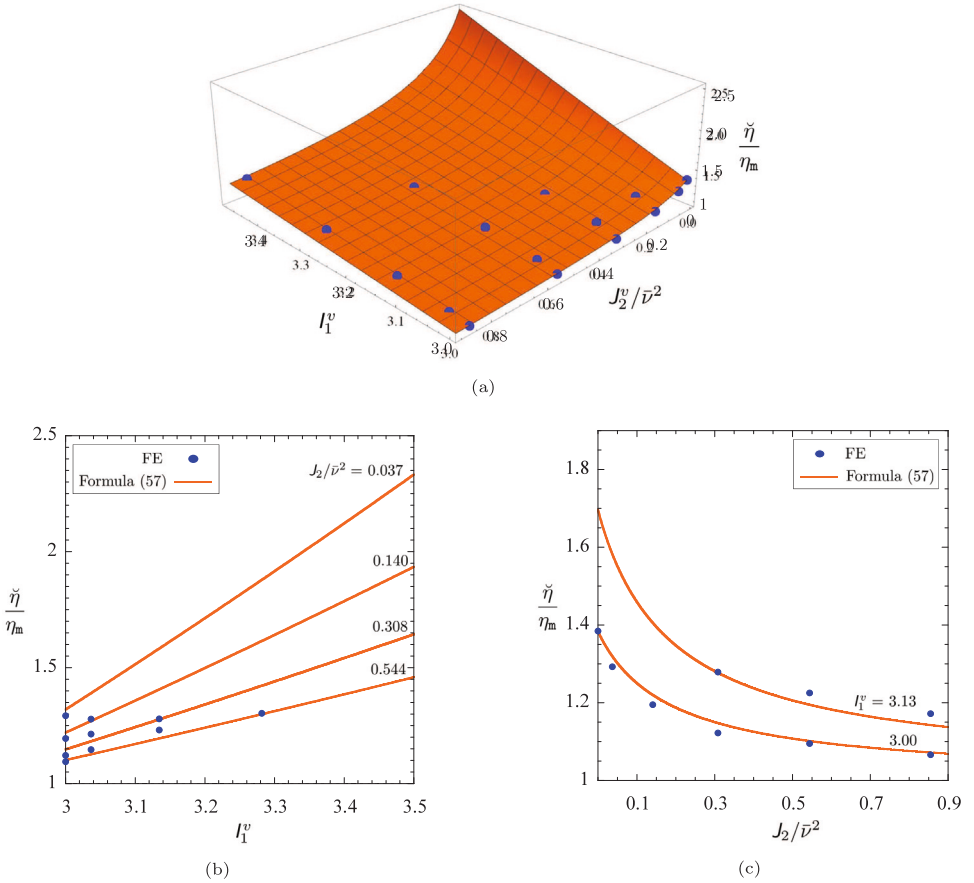

Fig. 7. The effective viscosity $\breve{\eta}$ for a suspension of monodisperse spherical inclusions at $c = 0.15$ volume fraction in a rubber matrix with material constants $\nu_m = \mu_m$, $\eta_m = \tau_m\nu_m$, $\tau_m = 1$ s. The results are shown normalized by the viscosity η_m of the rubber matrix as functions of the invariants I_1^v and J_2^v. The solid circles correspond to FE results while the solid surface in (a) and solid lines in (b)–(c) correspond to the proposed formula (58) with the pertinent fitted effective constants listed in Table 1, namely, $K_1/\mu_m = 2.740$, $K_2 = 0.520$, $K_3 = 0.909$, $\beta_1 = 0.975$, $\beta_2 = 1.619$, $\beta_3 = 0.540$.

Rather expediently, relation (74) states that the function $\breve{\eta}\left(I_1^v, J_2^v\right)$ for the effective viscosity can be evaluated at any desired values of its arguments by applying loading conditions of the form (72) with different choices of initial $\mathbf{F}_0$ and final $\mathbf{F}_1$ macroscopic deformation gradients and by computing the time derivative $\dot{\mathbf{S}}(t)$ of the resulting macroscopic stress $\mathbf{S}(t)$ at time $t = 0+$.

Fig. 7 presents a set of representative results for the effective viscosity $\breve{\eta}$ determined in the manner outlined above for a suspension of monodisperse spherical inclusions. The results pertain to a rubber matrix with material constants $\nu_{\mathrm{m}} = \mu_{\mathrm{m}}$, $\eta_{\mathrm{m}} = \tau_{\mathrm{m}}\nu_{\mathrm{m}}$, $\tau_{\mathrm{m}} = 1$ s, volume fraction of inclusions $c = 0.15$, and show the normalized effective viscosity $\breve{\eta}/\eta_{\mathrm{m}}$ as a function of the invariants I_1^v and J_2^v; while part (a) shows results in the entire (I_1^v, J_2^v)-space, parts (b) and (c) show results in terms of I_1^v for several fixed values of J_2^v and viceversa, respectively. Two observations are immediate. The first one is that $\breve{\eta}$ is a decreasing function of J_2^v. The other one is that $\breve{\eta}$ is an increasing function of I_1^v.

Computation of the effective material constants K_1, K_2, K_3, β_1, β_2, β_3 *in* (58). In addition to the results (solid circles) for the effective viscosity $\breve{\eta}$ obtained directly from FE computations, all three parts of Fig. 7 also include the results (solid surface and lines) given by the approximation (58) proposed in the main body of the text with effective material constants $K_1/\mu_{\mathrm{m}} = 2.740$, $K_2 = 0.520$, $K_3 = 0.909$, $\beta_1 = 0.975$, $\beta_2 = 1.619$, $\beta_3 = 0.540$. These values were obtained via a least-squares fit of the FE data with the formula (58). The computation of the effective material constants K_1, K_2, K_3, β_1, β_2, β_3 for a given suspension of interest amounts thus to first generating numerical results for the effective viscosity $\breve{\eta}\left(I_1^v, J_2^v\right)$ in the (I_1^v, J_2^v)-space in the manner outlined above and then fitting via least squares the formula (58) to those results thereby determining the corresponding values for K_1, K_2, K_3, β_1, β_2, β_3.

References

Amin, A.F.M.S., Lion, A., Sekita, S., Okui, Y., 2006. Nonlinear dependence of viscosity in modeling the rate-dependent response of natural and high damping rubbers in compression and shear: experimental identification and numerical verification. Int. J. Plast. 22, 1610–1657.

Avellaneda, M., 1987. Iterated homogenization, differential effective medium theory and applications. Commun. Pur. Appl. Math. 40, 527–554.

Batchelor, G.D., Green, J.T., 1972. The determination of the bulk stress in a suspension of spherical particles to order c^2. J. Fluid Mech. 56, 401–427.

Boehler, J.P., 1987. Applications of Tensor Functions in Solid Mechanics. Springer-Verlag.

Boffi, D., Brezzi, F., Fortin, M., 2012. Mixed Finite Element Methods and Applications. Springer, New York.

Brady, J.F., Bossis, G., 1988. Stokesian dynamics. Annu. Rev. Fluid Mech. 20, 111–157.

Brenner, R., Masson, R., Castelnau, O., Zaoui, A., 2002. A "quasi-elastic" affine formulation for the homogenised behaviour of nonlinear viscoelastic polycrystals and composites. Eur. J. Mech. A Solids 21, 943–960.

Brinkman, H.C., 1952. The viscosity of concentrated suspensions and solutions. J. Chem. Phys. 20, 571–573.

Brinson, L.C., Knauss, W.G., 1991. Thermorheologically complex behavior of multi-phase viscoelastic materials. J. Mech. Phys. Solids 39, 859–880.

Chi, H., Lopez-Pamies, O., Paulino, G.H., 2016. A variational formulation with rigid-body constraints for finite elasticity: Theory, finite element implementation, and applications. Comput. Mech. 57, 325–338.

Chockalingam, S., Roth, C., Henzel, T., Cohen, T., 2021. Probing local nonlinear viscoelastic properties in soft materials. J. Mech. Phys. Solids 146, 104172.

Cross, M.M., 1970. Kinetic interpretation of non-Newtonian flow. J. Colloid Interface Sci. 33, 30–35.

Doi, M., Edwards, S.F., 1998. The Theory of Polymer Dynamics. Oxford University Press, New York.

Einstein, A., 1906. Eine neue bestimmung der moleküldimensionen. [A new determination of molecular dimensions]. Ann. Physics 324, 289–306.

Francfort, G.A., Suquet, P., 1986. Homogenization and mechanical dissipation in thermoviscoelasticity. Arch. Ration. Mech. Anal. 96, 265–293.

Gent, A.N., 1962. Relaxation processes in vulcanized rubber. I. Relation among stress relaxation, creep, recovery, and hysteresis. J. Appl. Polym. Sci. 6, 433–441.

Ghossein, E., Lévesque, M., 2012. A fully automated numerical tool for a comprehensive validation of homogenization models and its application to spherical particles reinforced composites. Int. J. Solids Struct. 49, 1387–1398.

Girault, V., Raviart, P.-A., 1986. Finite Element Methods for Navier–Stokes Equations. Theory and Algorithms. Berlin.

Goudarzi, T., Spring, D.W., Paulino, G.H., Lopez-Pamies, O., 2015. Filled elastomers: A theory of filler reinforcement based on hydrodynamic and interphasial effects. J. Mech. Phys. Solids 80, 37–67.

Gross, B., 1953. Mathematical Structure of the Theories of Viscoelasticity. Hermann, Paris.

Gusev, A.A., 1997. Representative volume element size for elastic composites: A numerical study. J. Mech. Phys. Solids 45, 1449–1459.

Halphen, B., Nguyen, Q.S., 1975. Sur les matériaux standard généralisés. J. Mec. 14, 39–63.

Hashin, Z., 1963. Theory of mechanical behaviour of heterogeneous media. In: Technical Report. 3, Office of Naval Research, pp. 1–39.

Hashin, Z., 1965. Viscoelastic behavior of heterogeneous media. J. Appl. Mech. 32, 630–636.

Hashin, Z., 1970. Complex moduli of viscoelastic composites — I. General theory and application to particulate composites. Int. J. Solids Struct. 6, 539–552.

Hill, R., 1972. On constitutive macrovariables for heterogeneous solids at finite strain. Proc. R. Soc. London A 326, 131–147.

Hu, H.H., 1998. Numerical simulation of particle motion in viscoelastic fluids. IUTAM Symposium on Lubricated Transport of Viscous Materials 177–191.

Idiart, M.I., Lahellec, N., Suquet, P., 2020. Model reduction by mean-field homogenization in viscoelastic composites. Part 1: Primal theory. Proc. R. Soc. A. 476, 20200407.

Jeffrey, D.J., Acrivos, A., 1976. The rheological properties of suspensions of rigid particles. Am. Inst. Chem. Eng. J. 22, 417–432.

Khan, A.S., Lopez-Pamies, O., 2002. Time and temperature dependent response and relaxation of a soft polymer. Int. J. Plast. 18, 1359–1372.

Krieger, I.M., 1972. Rheology of monodisperse latices. Adv. Colloid Interface Sci. 3, 111–136.

Krieger, I.M., Dougherty, T.J., 1959. A mechanism for non-Newtonian flow in suspensions of rigid spheres. Trans. Soc. Rheol. 3, 137–152.

Kumar, A., Lopez-Pamies, O., 2016. On the two-potential constitutive modelling of rubber viscoelastic materials. Comptes Rendus MÉcanique 344, 102–112.

Lahellec, N., Suquet, P., 2007a. Effective behavior of linear viscoelastic composites: A time-integration approach. Int. J. Solids Struct. 44, 507–529.

Lahellec, N., Suquet, P., 2007b. On the effective behavior of nonlinear inelastic composites: I. Incremental variational principles. J. Mech. Phys. Solids 55, 1932–1963.

Lahellec, N., Suquet, P., 2007c. On the effective behavior of nonlinear inelastic composites: II. A second order-procedure. J. Mech. Phys. Solids 55, 1964–1992.

Lawson, J.D., 1966. An order five Runge–Kutta process with extended region of stability. SIAM J. Numer. Anal. 3, 593–597.

Lawson, J.D., 1967. An order six Runge–Kutta process with extended region of stability. SIAM J. Numer. Anal. 4, 620–625.

Le Tallec, P., Rahier, C., Kaiss, A., 1993. Three-dimensional incompressible viscoelasticity in large strains: formulation and numerical approximation. Comput. Methods Appl. Mech. Engrg. 109, 233–258.

Lefèvre, V., Garnica, A., Lopez-Pamies, O., 2019. A WENO finite-difference scheme for a new class of Hamilton–Jacobi equations in nonlinear solid mechanics. Comput. Methods Appl. Mech. Engrg. 349, 17–44.

Lefèvre, V., Lopez-Pamies, O., 2017a. Nonlinear electroelastic deformations of dielectric elastomer composites: I — Ideal elastic dielectrics. J. Mech. Phys. Solids 99, 409–437.

Lefèvre, V., Lopez-Pamies, O., 2017b. Nonlinear electroelastic deformations of dielectric elastomer composites: II — Non-Gaussian elastic dielectrics. J. Mech. Phys. Solids 99, 438–470.
Lefèvre, V., Lopez-Pamies, O., 2021. The effective shear modulus of a random isotropic suspension of monodisperse rigid n-spheres: From the dilute limit to the percolation threshold. In preparation.
Lévesque, M., Derrien, K., Mishnaevsky, L., Baptiste, D., Gilchrist, M.D., 2004. A micromechanical model for nonlinear viscoelastic particle reinforced polymeric composite materials—undamaged state. Compos. Part A: Appl. Sci. Manuf. 35, 905–913.
Li, J., Weng, G., 1997. A secant-viscosity approach to the time-dependent creep of an elastic-viscoplastic composite. J. Mech. Phys. Solids 45, 1069–1083.
Lopez-Pamies, O., Goudarzi, T., Danas, K., 2013b. The nonlinear elastic response of suspensions of rigid inclusions in rubber: II — A simple explicit approximation for finite-concentration suspensions. J. Mech. Phys. Solids 61, 19–37.
Lopez-Pamies, O., Goudarzi, T., Nakamura, T., 2013a. The nonlinear elastic response of suspensions of rigid inclusions in rubber: I — An exact result for dilute suspensions. J. Mech. Phys. Solids 61, 1–18.
Lubachevsky, B.D., Stillinger, F.H., 1990. Geometric properties of random disk packings. J. Stat. Phys. 60, 561–583.
Lubachevsky, B.D., Stillinger, F.H., Pinson, E.N., 1991. Disks vs. spheres: Contrasting properties of random packings. J. Stat. Phys. 64, 501–523.
Michel, J.C., Moulinec, H., Suquet, P., 1999. Effective properties of composite materials with periodic microstructure: a computational approach. Comput. Methods Appl. Mech. Eng. 172, 109–143.
Miehe, C., Schotte, J., Lambrecht, M., 2002. Homogenization of inelastic solid materials at finite strains based on incremental minimization principles. Application to the texture analysis of polycrystals. J. Mech. Phys. Solids 50, 2123–2167.
Norris, A., 1985. A differential scheme for the effective moduli of composites. Mech. Mater. 4, 1–16.
Pallicity, T.D., Böhlke, T., 2021. Effective viscoelastic behavior of polymer composites with regular periodic microstructures. Int. J. Solids Struct. 216, 167–181.
Reese, S., Govindjee, S., 1998. A theory of finite viscoelasticity and numerical aspects. Int. J. Solids Struct. 35, 3455–3482.
Roscoe, R., 1952. The viscosity of suspensions of rigid spheres. Br. J. Appl. Phys. 3, 267–269.
Roters, F., Eisenlohr, P., Hantcherli, L., Tjahjanto, D.D., Bieler, T.R., Raabe, D., 2010. Overview of constitutive laws, kinematics, homogenization and multiscale methods in crystal plasticity finite-element modeling: Theory, experiments, applications. Acta Mater. 58, 1152–1211.
Sanchez-Palencia, E., 1980. Non homogeneous media and vibration theory. In: Springer-Verlag Monograph in Physics. 127, Berlin-Heidelberg-New York.
Schöberl, J., 1997. NETGEN an advancing front 2D/3D-mesh generator based on abstract rules. Comput. Visual. Sci. 1, 41–52.
Scott, G.D., 1960. Packing of spheres: Packing of equal spheres. Nature 188, 908–909.
Segurado, J., Llorca, J., 2002. A numerical approximation to the elastic properties of sphere-reinforced composites. J. Mech. Phys. Solids 50, 2107–2121.
Shrimali, B., Lefèvre, V., Lopez-Pamies, O., 2019. A simple explicit homogenization solution for the macroscopic elastic response of isotropic porous elastomers. J. Mech. Phys. Solids 122, 364–380.
Shu, C.-W., Osher, S., 1988. Efficient implementation of essentially non-oscillatory shock capturing schemes. J. Comput. Phys. 77, 439–471.
Sidoroff, F., 1974. Un modèle viscoélastique non linéaire avec configuration intermédiaire. J. Mec. 13, 679–713.
Sierou, A., Brady, J.F., 2001. Accelerated Stokesian dynamics simulations. J. Fluid Mech. 448, 115–146.
Simo, J.C., 1992. Algorithms for static and dynamic multiplicative plasticity that preserve the classical return mapping schemes of the infinitesimal theory. Comput. Methods Appl. Mech. Eng. 99, 61–112.
Spinelli, S.A., Lefèvre, V., Lopez-Pamies, O., 2015. Dielectric elastomer composites: A general closed-form solution in the small-deformation limit. J. Mech. Phys. Solids 83, 263–284.
Stickel, J.J., Powell, R.L., 2005. Fluid mechanics and rheology of dense suspensions. Annu. Rev. Fluid Mech. 37, 129–149.
Suquet, P., 1987. Elements of homogenization for inelastic solid mechanics. In: Sanchez-Palencia, E., Zaoui, A. (Eds.), Homogenization Techniques for Composite Media. Lecture Notes in Physics. 272, Springer, New York, pp. 193–278.
Treloar, L.R.G., 1975. The Physics of Rubber Elasticity. Oxford University Press, Oxford.
Willis, J.R., 1981. Variational and related methods for the overall properties of composites. Adv. Appl. Mech. 21, 1–78.
Yeong-Moo, Y., Sang-Hoon, P., Sung-Kie, Y., 1998. Asymptotic homogenization of viscoelastic composites with periodic microstructures. Int. J. Solids Struct. 35, 2039–2055.
Zener, C.M., 1948. Elasticity and Anelasticity of Metals. University of Chicago Press, Chicago.
Ziegler, H., Wehrli, C., 1987. The derivation of constitutive relations from the free energy and the dissipation function. Adv. Appl. Mech. 25, 183–238.